Orbiting Carbon Observatory-2 & -3 (OCO-2 & OCO-3)

Retrievals of Carbon Dioxide from GOSAT Using the Atmospheric CO_2 Observations from Space (ACOS) Algorithm Level 2 Standard Product and Lite Data Product Data User's Guide, v9

Version 2.0 Revision A
March 25, 2020

National Aeronautics and
Space Administration

Jet Propulsion Laboratory
California Institute of Technology
Pasadena, California

Prepared By:

Christopher O'Dell, CSU
Orbiting Carbon Observatory-2 (OCO-2), Orbiting Carbon Observatory-3 (OCO-3) Algorithm Teams

Gregory Osterman, JPL
OCO-2, OCO-3 Science Validation Teams

Annmarie Eldering, JPL
OCO-3 Project Scientist
OCO-2 Deputy Project Scientist

Cecilia Cheng, JPL
OCO-3 Mission Operations Manager
OCO-2 Science Data Operations System Manager

David Crisp, JPL
OCO-2 Science Team Lead

Christian Frankenberg, California Institute of Technology
OCO-2 Algorithm Team

Brendan Fisher, JPL
OCO-3, OCO-2 Algorithm and Validation Teams

The research described in this document was carried out at the Jet Propulsion Laboratory, California Institute of Technology, under a contract with the National Aeronautics and Space Administration.

Revision History

Revision Date	Changes	Author
1 October 2010	Initial Release	C. Avis
20 December 2010	Updates to most sections including changes to ACOS metadata/elements based on the v2.8.00 delivery. Updated quality provided by G.Osterman.	E. Martinez
30 October 2011	Complete revision of document. Includes updates for Build 2.9	E. Martinez
29 November 2011	Rev B: Updated links to Mirador, corrected typos	E. Martinez
7 December 2011	Rev C: corrected typo on page 17 and added additional instructions on how to get data in section 4. ACOS release v2.9	E. Martinez
26 October 2012	Rev D: Updated to further describe experience with v130130 data, and the preliminary experience with v15015x. Additional information about biases between Gain H and Gain M has been added. Errors associated with geolocation uncertainties also added. ACOS release v2.9	D. Crisp
29 October 2012	Rev E: Updated for ACOS release v2.10	C. O'Dell, G. Osterman, A. Eldering, D. Crisp, C. Avis
15 April 2013	Rev F: Updated for ACOS release v3.3	C. O'Dell, G. Osterman, B. Fisher, C. Frankenberg, C. Avis
3 October 2013	Rev A: Updated for ACOS release v3.4	C. O'Dell, G. Osterman, A. Eldering
26 November 2013	Rev B: Updated for version 3.4 release-2	C. O'Dell, A. Eldering
3 January 2014	Rev C: Fixed minor typos and mistakes in bias-correction coefficients	C. O'Dell
18 March 2014	Rev D: Updated for version 3.4 release-3	C. O'Dell
14 July 2014	Rev A : Updated for ACOS release v3.5	C. O'Dell
24 July 2014	Rev B : Slight change to filtering and bias correction for v3.5	C. O'Dell
5 May 2015	Rev C : Updated to release-2 bias correction for v3.5	C, O'Dell
28 March 2016	Rev D : Minor updates to this guide to reflect latest literature and guidance, table updates to reflect v3.5 product	C. O'Dell, C. Avis G. Osterman
12 January 2017	Rev E: Updated for v7.3 release of the ACOS data product and description of the Lite data files	G. Osterman, A. Eldering, C. O'Dell

Revision Date	Changes	Author
19 October 2017	Rev F: Fix a typo in the description of the XCO2 vs XCO2_raw fields	G. Osterman
25 March 2020	Version 2.0 Rev A: Updated for ACOS release v9	C. O'Dell, G. Osterman

Table of Contents

1. Introduction 8
1.1. Scope and Background 8
1.2. Overview of Document 8
1.3. Data Usage Policy 8
2. V9 ACOS L2 Data Products 9
2.1. Differences Between v7.3 and v9 9
2.2. Validation Status 9
2.3. Data Description and User Alerts 10
2.3.1. Data Completeness/Coverage 10
2.3.2. Chlorophyll Fluorescence 10
2.3.3. Cloud-Screening 10
2.3.4. Pre-Processing for v9 11
2.3.5. Post-Processing 12
2.3.6. Quality Flagging 12
2.3.7. Averaging Kernels 12
2.3.8. Known Problems 12
2.4. Key Science Data Fields 12
2.4.1. RetrievalResults/xco2 12
2.4.2. SoundingHeader/cloud_flag 12
2.4.3. RetrievalResults/surface_pressure_fph 13
2.5. Science Analysis Recommendations 13
2.5.1. Differences among releases 13
2.5.2. Recommended Data Screening 13
2.5.3. Aerosol and cloud variables filter variables 14
2.5.4. Other filter variables 15
2.5.5. Recommended Bias Correction 18
2.5.6. V9 (first release) bias correction (recommended) 18
2.5.7. Model-data comparisons and application to flux inversions 21
2.5.8. GOSAT H- and M-Gain Data 22
3. Background Reading 22
3.1. About the GOSAT Mission 22
3.1.1. Instrument 22
3.1.2. Orbital Parameters 23
3.1.3. Path ID Definition 23
3.2. GOSAT L1B Releases 24
3.3. About the ACOS Task 24
3.4. ACOS Algorithms 27
3.4.1. Level 1B Algorithm Overview 27
3.4.2. Level 2 Algorithm Overview 27
3.5. ACOS Data Products – L2 Standard Data 29

3.5.1. File Naming Convention 29
3.5.2. File Format and Structure 30
3.5.3. Data Definition 30
3.5.4. Global Attributes 30
3.5.5. ACOS L2 Standard Data Tables and Fields 31
4. ACOS Level 2 Lite Data Products 51
5. Tools and Data Services 55
5.1. HDFView 55
5.2. Panoply. 55
5.3. Goddard DAAC user interface. 55
5.4. NASA Earth Data Search Client 55
6. Contact Information 57
7. Acknowledgements, References and Documentation 58
7.1. Acknowledgements 58
7.2. Links 58
7.3. References 58
7.3.1. GOSAT 58
7.3.2. OCO-2 Mission 58
7.3.3. Algorithms and Retrievals 60
7.3.4. Chlorophyll Fluorescence 61
7.3.5. Validation and TCCON 61

Table of Figures

Figure 1: Hovmöller plot of the ACOS/GOSAT data for the time period 2009-2019. The plot shows how the global coverage moves North/South over the course of a year (more noticeable in the Northern Hemisphere). Figure also shows the growth in XCO2 over the course of the observations. 11
Figure 2: Plot showing the land gain H filtering process, without (black) and with (light blue) bias correction. Each panel shows the mean bias of the retrieved X_{CO2} as evaluated against TCCON for the v9 dataset. The figure should be read left-to-right, top-to-bottom. Each panel shows the effect of a filter variable, applied cumulatively to all the variables that came before it. In the top right corner of each panel is displayed the number of surviving soundings after that filter has been applied (again, cumulatively), and the standard deviation of the X_{CO2} errors for those soundings surviving to that point. The dark blue diamonds show the standard deviation of the X_{CO2} error in each bin. 17
Figure 3: ACOS/GOSAT XCO2 data for February 2017 after screening. 20
Figure 4: GOSAT Observation Concept. 23
Figure 5: GOSAT TANSO-FTS Observation Details. 24
Figure 6: Level 2 Full Physics Retrieval Flow 29

Table of Tables

Table 1: Screening criteria for v9 level-2 XCO2 retrievals....13
Table 2: v9 bias correction parameters and their estimated uncertainties. 20
Table 3: Description of the different GOSAT L1B releases. 25
Table 4: Some Global Metadata Attributes 31
Table 5: Key Metadata Fields....31
Table 6: Metadata Information 31
Table 7: Spacecraft Geometry Variables (Spacecraft Geometry) 34
Table 8: Sounding Geometry Variables (SoundingGeometry) 35
Table 9: Sounding Header Variables (SoundingHeader) 36
Table 10: A-Band-only Retrieval Variables (ABandCloudScreen) 36
Table 11: IMAP-DOAS Retrieval Variables (IMAPDOASPreprocessing)....37
Table 12: Retrieval Header Variables (RetrievalHeader)....38
Table 13: Variables Expressing Retrieval Results (RetrievalResults)....39
Table 14: Spectral Parameter Variables....43
Table 15: Bit Flag Definitions 44
Table 16: Fields in the Aerosol Results group of the L2 data products (AerosolResults) 45
Table 17: Fields in the Albedo Results group of the L2 data products (AlbedoResults) 45
Table 18: Fields in the BRDF Results group of the L2 data products (BRDFResults)....46
Table 19: Fields in the Dispersion Results group of the L2 data products (DispersionResults) 48
Table 20: Fields in the IMAP DOAS Preprocessing Results group of the L2 data products (IMAPDOASPreprocessingResults)....48
Table 21 provides a description of the fields in the ACOS Lite Data Product files.....51
Table 22 Contains description of the fields in the "Preprocessor" folder of the Lite files. 52
Table 23 Contains description of the fields in the "Retrievals" folder of the Lite files. 52
Table 24 Contains description of the fields in the "Sounding" folder of the Lite files. 54
Table 25: Fields in the "Meteorology" folder of the ACOS/GOSAT Lite files. 54

1. Introduction

1.1. Scope and Background

This document provides an overview of the v9 (sometimes called B9; they are the same) Atmospheric CO_2 Observations from Space (ACOS) data product, key features and issues, preliminary validation information, recommendations on data usage, as well as background on the Greenhouse Gases Observing Satellite (GOSAT) mission measurements and the ACOS algorithm. The later sections provide the reader with information on filename conventions and a detailed guide to the format and fields in the hdf product.

This is the eighth 'public release' of ACOS data, the previous released version being v7.3, which was released in 2016. The ACOS v2.10 data were unofficially released in October 2012. The v2.8 and v2.9 data are described in a series of validation papers published in 2011 and 2012. This document updates findings from these papers for v9, and gives more general information on the use of ACOS data.

While Build 9 is now relatively mature, the Build 9 (v9) retrievals continue to be evaluated, and the guidance provided herein may be incomplete. Version 9 is the latest version of the ACOS data to be released after the launch of the Orbiting Carbon Observatory-2 (OCO-2) in July 2014. The retrieval algorithm used to create the Build 9 ACOS data product is consistent with that used to create the OCO-2 v9 data product, described at length in O'Dell et al. (2018). This allows comparison of the ACOS and OCO-2 data without having to consider algorithm differences.

1.2. Overview of Document

The remainder of this section describes the usage of the ACOS data. Section 2 provides details of the differences in this version, product characteristics, validation status, key data fields and ends with recommendations for data analysis. Section 3 provides background information on the GOSAT mission, ACOS file and data conventions, and a complete listing of metadata elements in the v9 ACOS data product. Section 4 lists tools to view and search the data products. Section 5 lists contact information for both GOSAT and ACOS data, and the last section lists acknowledgements and relevant publications.

1.3. Data Usage Policy

This data has been produced by the ACOS project, and is provided freely to the public. The ACOS project has been made possible by the generous collaboration with our Japanese colleagues at Japanese Aerospace Agency (JAXA), National Institute for Environmental Studies (NIES), and the Ministry of the Environment (MOE). The Level 1 GOSAT data have been made available for this project through an agreement between the GOSAT Three Parties and Caltech. In order to improve our product and receive continued support for this work, we need user feedback and also have users properly acknowledge data usage. Therefore, we request that when publishing using ACOS data; please acknowledge NASA and the ACOS/OCO-2 project.

Include OCO-2 as a keyword to facilitate subsequent searches of bibliographic databases if it is a significant part of the publication

Include a bibliographic citation for ACOS/OCO-2 data. The most relevant citations currently are O'Dell et al. (2018) and Wunch et al. (2017).

Include the following acknowledgements: "These data were produced by the ACOS/OCO-2 project at the Jet Propulsion Laboratory, California Institute of Technology, and obtained from the JPL website, co2.jpl.nasa.gov."

Include an acknowledgement to the GOSAT Project for acquiring these spectra.

We recommend sending courtesy copies of publications to the OCO-2 Project Scientist, Michael.R.Gunson@jpl.nasa.gov.

2. V9 ACOS L2 Data Products

2.1. Differences Between v7.3 and v9

Changes to the L2 products are as follows:

- Changes to input or ancillary data used to process the L2 products
- New versions of the GOSAT L1B data. From April 2009 through February 2018, v205205 of the L1B data was used. April 2018 onward uses v210210 (see "Release Notes for GOSAT FTS Level 1 Products (Ver.210.210)", 2018). At the time of this writing, the latest official GOSAT L1B product is v220220.
    - Updates for GOSAT L1B v210210 include
        - Modification of Band 4 TIR non-linearly correction to improve long term radiometric calibration consistency.
        - Extension of sun-glint latitudinal range and glint flag updates.
        - Update of SWIR radiance conversion table.
        - Change of Band1 high gain saturation criteria.
        - Update of Quality Flag: poor data detection algorithm
- Within the code (many of these changes make the code used for ACOS v9 data processing consistent with that used for OCO-2 v9)
    - Use ABSCO 5.0 (v7 used ABSCO 4.2)
    - Use GEOS5 FP-IT instead of ECMWF for the prior meteorology
    - Inclusion of a stratospheric aerosol type in the retrieval
    - Updates to bias correction and screening recommendations
    - Explicit filtering & bias correction for land gain M data (ACOS B7.3 did not include filtering or bias correction recommendations for land gain M)

2.2. Validation Status

The v9 ACOS X_{CO2} data product has undergone a *preliminary* validation against both TCCON data and atmospheric models. Detailed comparisons of previous ACOS versions to TCCON have been published in Wunch et al. (2011b), Lindqvist et al. (2015) and Kulawik et al. (2016). More work is being done to inter-compare the ACOS v9, OCO-2 v9 and TCCON data.

2.3. Data Description and User Alerts

2.3.1. Data Completeness/Coverage

GOSAT L1B Version 205205/210210 was used for all L2 retrievals in v9.

The first three months of GOSAT operations (April-May, 2009) have incomplete operational coverage due to on-orbit calibrations and checkout activities. Full coverage begins about 1 July 2009. Users should exercise caution when using any data before 1 July 2009.

Typically, data products contain 10-200 useful soundings per orbit, out of the 600-700 L1B soundings collected in an orbit. Note that over 50% of the data is not processed because it does not pass the first cloud screening pre-processing step. A large fraction of data is collected over ocean but not in glint, and thus is not processed. Of the ~100 soundings that are processed for each orbit, convergence and quality screens identify about 50% of that data as good.

If data users create maps of the filtered v9 carbon dioxide data, they should expect to see glint measurements move north and south during the year. Figure 1 shows a Hovmöller plot of the ACOS v9 X_{CO2} data, illustrating how the increase in carbon dioxide over the observation record and changes in the observation coverage in the Northern hemisphere.

2.3.2. Chlorophyll Fluorescence

Since ACOS v3.3, solar-induced chlorophyll fluorescence (SIF) is included in the full-physics code as an additional state vector element. This is true for v9 as well and the main motivation for this is to reduce a potential bias on XCO_2, as outlined in detail in Frankenberg et al. (2012). This product, however, should not be used to look at chlorophyll fluorescence itself, as there is a high interference with other state vector elements (surface pressure, albedo, aerosols). Fluorescence is NOT fit for in gain M data over land, which is primarily non-vegetated desert, as well as ocean data, where the ocean fluorescence signal from phytoplankton is expected to be small. The SIF product included in the ACOS data products should not be used

The IMAP-DOAS preprocessor performs fluorescence retrievals using Fraunhofer lines only, which is more robust and should be used as the ACOS fluorescence product. However, the fields reported in the official level 2 file have not yet been optimally corrected for the 0-level offset observed in GOSAT O2 A-band spectra (Frankenberg et al, 2011). A separate unofficial fluorescence dataset (monthly ascii files of single soundings) will be available upon request (contact is Christian Frankenberg cfranken@caltech.edu).

2.3.3. Cloud-Screening

To further reduce the computation time of retrievals containing clouds, the cloud screening algorithm is applied to this version. It performs a fast, Oxygen A-band only clear-sky retrieval for surface pressure, surface albedo, temperature offset and dispersion multiplier. The retrieved surface pressure and albedo information are combined with the χ^2 goodness-of-fit statistic and signal-to-noise ratio to determine if a scene is clear(0), cloudy (1), or skipped (2). The difference of this retrieved surface pressure with respect to the prior (GEOS5 FP-IT) analysis-based estimate serves as the chief filter criterion; this difference must be less than 25 hPa for the sounding to pass the screen. See Taylor et al. (2012, 2017) for further details on the Oxygen A-band cloud-screening algorithm.

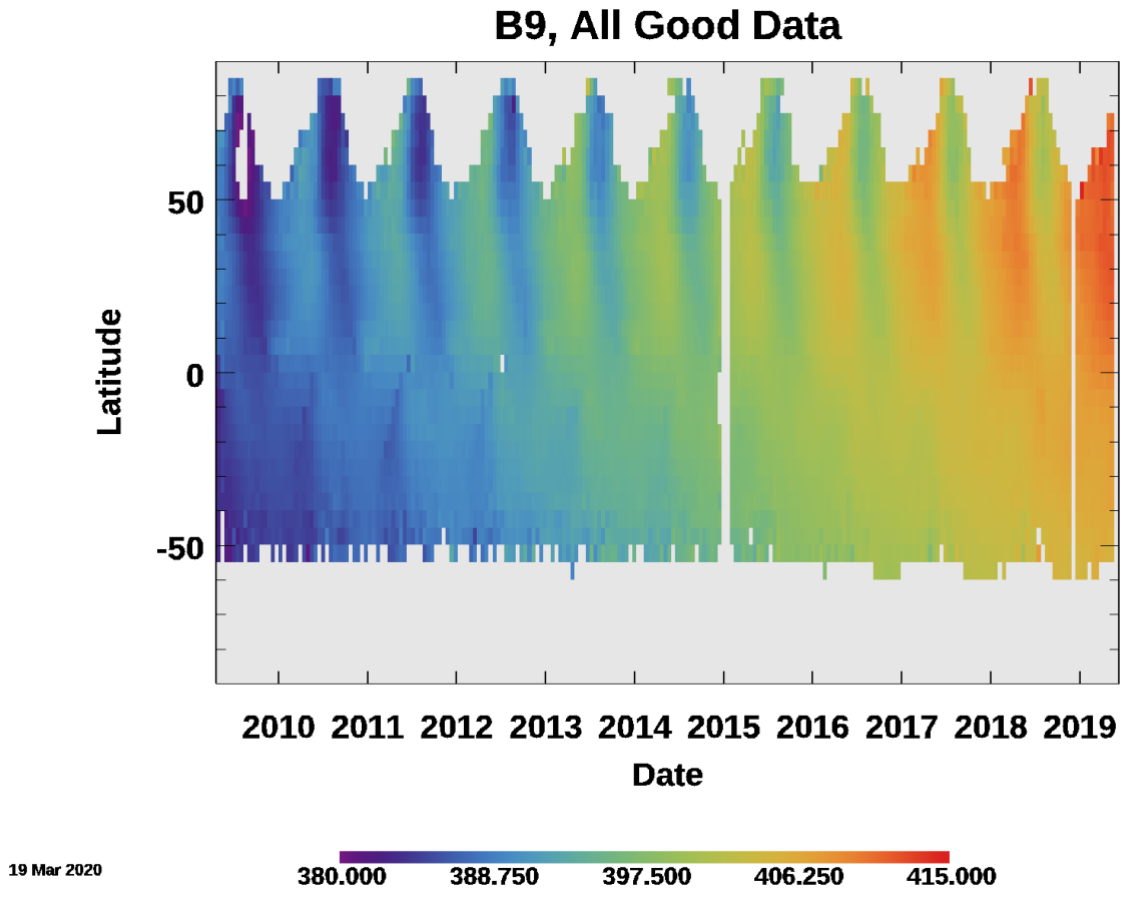

Figure 1: Hovmöller plot of the ACOS/GOSAT data for the time period 2009-2019. The plot shows how the global coverage moves North/South over the course of a year (more noticeable in the Northern Hemisphere). Figure also shows the growth in XCO2 over the course of the observations.

2.3.4. Pre-Processing for v9

The v9 preprocessing is the same as that for versions v7.3 and v3.5. In version v3.5, a preprocessing scheme was used that is similar to that used for the v3.3 (and earlier) ACOS data version. This is in contrast to v3.4, which used additional pre-filters to speed up processing. This additional processing speed was not necessary for v9, so only a mild cloud-screen was used (see above). In the case of soundings over water, a check was made to ensure the observation was made in glint mode.

2.3.5. Post-Processing

No bias correction – the retrieval results in the standard HDF files have not been systematically corrected based upon some known reference source. Bias corrected XCO2 values are provided in the ACOS v9 "Lite" files.

No post-screening – the results in the standard HDF files include all soundings whose retrieval did not crash or exit with an error status. This means that even some non-converged soundings are present in the standard HDF files.

No post-processing filter has been applied to eliminate soundings based upon certain criteria.

2.3.6. Quality Flagging

There are several quality flags among the variables. The user should weigh the following information about the flags:

- *Retrieval_header/sounding_qual_flag* – quality of input data provided to the retrieval processing
- *Retrieval_results/outcome_flag* – retrieval quality based upon certain internal thresholds, which mainly describes where a sounding converged (outcome_flag =1 or 2), or failed to converge (outcome_flag=3 or 4).

2.3.7. Averaging Kernels

The data files include a column averaging kernel value for each retrieved sounding.

The normalized Averaging Kernel (*retrieval_results/xco2_avg_kernel_norm*) for a given pressure level is equal to the non-normalized value (*retrieval-results/xco2_avg_kernel*) divided by the pressure weighting function at that level. Note that levels are "layer boundaries" and have no thickness.

2.3.8. Known Problems

- Pointers to other files (e.g., '*InputPointer*') are not useful because those files reside only on the originating system and were not delivered to the GES DISC.

2.4. Key Science Data Fields

2.4.1. RetrievalResults/xco2

The Level 2 Standard Product contains the variable X_{CO2}. This variable expresses the column-averaged CO_2 dry air mole fraction for a sounding. These values are determined by a full-physics retrieval and have units of mol/mol.

2.4.2. SoundingHeader/cloud_flag

The Level 2 Standard Product contains the variable cloud_flag. This variable expresses the result of an analysis of cloud contamination within a sounding. Every sounding of a granule will have a value: 0 (Clear), 1 (Cloudy) or 2 (Undetermined). The values are determined by an ABO2-band-only retrieval using the FTS spectrum. The only soundings that will be processed by the L2 software are those with a value of 0 (Clear). However, this does NOT mean that all processed soundings are actually clear. Some cloudy scenes are invariably missed by the ABO2-only preprocessor, but can lead to bad XCO2 retrievals. Therefore, users are strongly encouraged to further apply the recommended quality filters given in section 2.5.2.

2.4.3. RetrievalResults/surface_pressure_fph

The Level 2 Standard Product contains the variable *surface_pressure_fph*. This variable expresses the retrieved atmospheric pressure at the Earth's surface for a given sounding. Those soundings that did not converge will not be present. These values are determined by a full-physics retrieval and have units of Pascals.

2.5. Science Analysis Recommendations

2.5.1. Differences among releases

This represents the first release of the filtering and bias correction for the v9 retrievals. The filters are similar but not identical to those users for the previous version, v7.3.

2.5.2. Recommended Data Screening

We now describe the recommended filters for science data screening. Good soundings will be those that pass all the criteria in Table 1. Note that these screenings, while similar, are distinctly different from that of v7.3. Therefore the screening for v9 should be used on v9 retrievals.

Table 1: Screening criteria for v9 level-2 XCO2 retrievals

Level 2 Standard File Variable Name	Lite File Variable Name	Ocean Glint	Land Gain H	Land Gain M
RetrievalResults/outcome_flag	N/A	1 or 2	1 or 2	1 or 2
RetrievalResults/aerosol_total_aod	Retrieval/aod_total	< 0.5	0.02 to 0.3	< 0.40
OD_Ice_Cloud	Retrieval/aod_ice	< 0.07	<0.06	0.002 to 0.05
AOD SO	Retrieval/aod_sulfate		< 0.20	
AOD ST	Retrieval/aod_strataer			0.0008 to 0.015
DWS (=AOD DU + SS + Water_Cloud)	Retrieval/dws			1e-4 to 0.35
AOD OC + SO (=AOD Fine)	Retrieval/aod_fine	< 0.18		< 0.04
Ice_Height	Retrieval/ice_height	-0.50 to 0.40	-0.12 to 0.40	-0.12 to 0.30
DU Height	Retrieval/dust_height		0.75 to 1.4	0.80 to 1.4
IMAPDOASPreprocessing/co2_ratio_idp	Preprocessors/co2_ratio	0.989 to 1.02	0.95 to 1.02	0.989 to 1.012
IMAPDOASPreprocessing/h2o_ratio_idp	Preprocessors/h2o_ratio		0.80 to 1.04	0.88 to 1.05
$\Delta P_{s,cld}$ [hPa]	Preprocessors/dp_abp	-25.0 to 14.0	-7.0 to 7.0	-10.0 to 7.0
RetrievalResults/xco2_uncert • 10_6 [ppm]	xco2_uncertainty		< 2.0	< 1.5
SoundingGeometry/sounding_altitude_stddev [m]	Sounding/altitude_stddev		< 250.0	< 250.0

Level 2 Standard File Variable Name	Lite File Variable Name	Ocean Glint	Land Gain H	Land Gain M
RetrievalResults/co2_grad_del [ppm]	Retrieval/co2_grad_del	-19.0 to 10.0	-40 to 100	-10 to 100
ΔP_s [hPa]	Retrieval/dp	-0.75 to 5.5	-2.0 to 10.0	-6.0 to 5.0
s32	Retrieval/s32	> 0.58		
RetrievalResults/albedo_weak_co2_fph	Retrieval/albedo_wco2	0.017 to 0.030		
RetrievalResults/brdf_reflectance_strong_co2_fph	Retrieval/albedo_sco2		0.04 to 1.0	0.10 to 1.0
RetrievalResults/albedo_slope_o2	Retrieval/albedo_slope_o2a		-4e-5 to 2e-5	
RetrievalResults/albedo_slope_weak_co2	Retrieval/albedo_slope_wco2	0.3e-5 to 2.75e-5		
RetrievalResults/albedo_slope_strong_co2	Retrieval/albedo_slope_wco2	0.0 to 5e-5	-1e-4 to 2.5e-4	
SpectralParameters/reduced_chi_squared_o2_fph	Retrieval/chi2_o2a		< 1.2	< 1.25
SpectralParameters/reduced_chi_squared_weak_co2_fph	Retrieval/chi2_wco2	< 1.40		< 1.40
SpectralParameters/reduced_chi_squared_strong_co2_fph	Retrieval/chi2_sco2	< 1.35		< 1.90
Offset_o2a_rel	Retrieval/offset_o2a_rel			-1.5 to 0.1
RetrievalResults/temperature_offset_fph	Retrieval/deltaT		-1.0 to 10.0	-0.7 to 1.2
RetrievalResults/eof_3_scale_o2	Retrieval/eof1_3	-0.05 to 0.04		
RetrievalResults/eof_2_scale_strong_co2	Retrieval/eof3_2	-0.15 to 0.35		
RetrievalResults/wind_speed [m/s]	Retrieval/windspeed	2 to 24		
Airmass	Sounding/airmass	< 3.0		

Some variables in the table must be constructed directly by users of the standard L2s HDF-5 files. All these variables should appear directly in the "Lite" files.

2.5.3. Aerosol and cloud variables filter variables

Because of the new variable aerosol types retrieved, extracting the amount of optical depth in each species is a bit trickier than in previous versions. For each sounding, there are four species of scatterers retrieved:

- Aerosol type 1. May be type dust (DU), sulfate (SO), OC (Organic Carbon), black carbon (BC), or sea salt (SS).
- Aerosol type 2. May be DU, SO, OC, BC, or SS, and will be different from aerosol type 1.
- Ice cloud
- Water cloud
- Stratospheric Aerosol (ST)

The HDF-5 files specify the fitted AOD and height for each species in terms of their number (1-4). Additionally, the variable "RetrievalResults/aerosol_types" indicates which type each aerosol corresponds to for a given sounding.

The following variables can then be constructed for use in the filtering. Some may also be needed for the bias correction.

- ***AOD_Sulfate.*** Find each sounding for which "aerosol_types" equals "SO". For each such sounding, the AOD due to sulfate is simply "Retrievalresults/aerosol_X_aod", where X is either type 1 or 2.
- ***AOD_Dust.*** As for *AOD_Sulfate*, but the AOD where "aerosol_types" equals "DU".
- ***AOD_SeaSalt.*** As for *AOD_Sulfate*, but the AOD where "aerosol_types" equals "SS".
- ***AOD_Water_cloud*** Because Water cloud is always retrieved, and it always occurs as type 4 in version v7, the retrieval optical depth (OD) due to Water cloud is simply:

$$\boldsymbol{OD\_Water\_Cloud} = RetrievalResults/aerosol\_4\_aod$$

- ***OD_Ice_cloud.*** Because Ice cloud is always retrieved, and it always occurs as type 3 in version v7, the retrieval optical depth (OD) due to Ice cloud is simply:

$$\boldsymbol{OD\_Ice\_Cloud} = RetrievalResults/aerosol\_3\_aod$$

- ***Ice_Height*** is the central pressure location of the retrieved ice cloud type, relative to the surface pressure. It has values typically between 0 and 1, though it can go slightly negative. It is the ***second*** element of the vector:

$$\boldsymbol{Ice\_Height} = RetrievalResults/aerosol\_3\_gaussian\_log\_param$$

2.5.4. Other filter variables

- $\boldsymbol{\Delta P_s}$ is the difference of the retrieved and prior surface pressure, given in hPa. It is constructed as

$$\boldsymbol{\Delta P_s} = (P_{s,retrieved} - P_{s,prior}) * 0.01$$

where $P_{s,retrieved}$ is the retrieved surface pressure *RetrievalResults/surface_pressure_fph* and $P_{s,prior}$ is the prior (meteorological) surface pressure from ECMWF (*RetrievalResults/surface_pressure_apriori_fph*).

- $\boldsymbol{\Delta P_{s,cld}}$ is the difference of the retrieved and prior surface pressure from the A-band cloud-screen, expressed in hPa:

$$\boldsymbol{\Delta P_{s,cld}} = ABandCloudScreen/surface\_pressure\_delta\_cloud \cdot 0.01$$

- ***Grad***$_{co2}$ is the difference in retrieved CO2 dry-air mole fraction between the surface and vertical level 13. Vertical level 13 is the level with *P/Psurf* = 12/19 = 0.631579. This is about 630 hPa for sounding elevations near sea level. This variable is something like a "lapse rate for CO2". High positive or negative values of this variable are indicative of poor soundings.
- ***ΔGrad***$_{co2}$ is the change in ***Grad***$_{co2}$ for the retrieved value with respect to the *a priori* value. It is essentially how much the "lapse rate for CO_2" has changed from the prior value to the retrieved value, and also can be indicative of bad soundings. The CO_2 profile for the prior is stored in *RetrievalResults/co2_profile_apriori*, and the retrieved profile is stored in *RetrievalResults/co2_profile*.
- ***DWS*** is the sume of the retrieved optical depths of Dust, Water cloud, and Sea Salt. From the definitions given above, it is then:

$$DWS = AOD\_Dust + AOD\_SeaSalt + OD\_Water\_cloud$$

- ***AOD_fine*** is the sume of the retrieved optical depths of organic carbon and sulfate. From the definitions given above, it is then:

$$DWS = AOD\_OC + AOD\_Sulfate$$

- ***S32*** is the ratio of the signal_sco2 to signal_wco2. These can be obtained from SpectralParameters/signal_strong_co2_fph and SpectralParameters/signal_weak_co2_fph, respectively.
- ***Offset_o2a_rel*** is a scaled version of the retrieved zero level offset in the o2a band:

$$Offset\_o2a\_rel = (RetrievalResults/zero\_level\_offset\_o2\_fph) / (1e7 * SpectralParamters/signal\_o2\_fph)$$

Figure 2 illustrates the filtering process for land, gain H ACOS data.

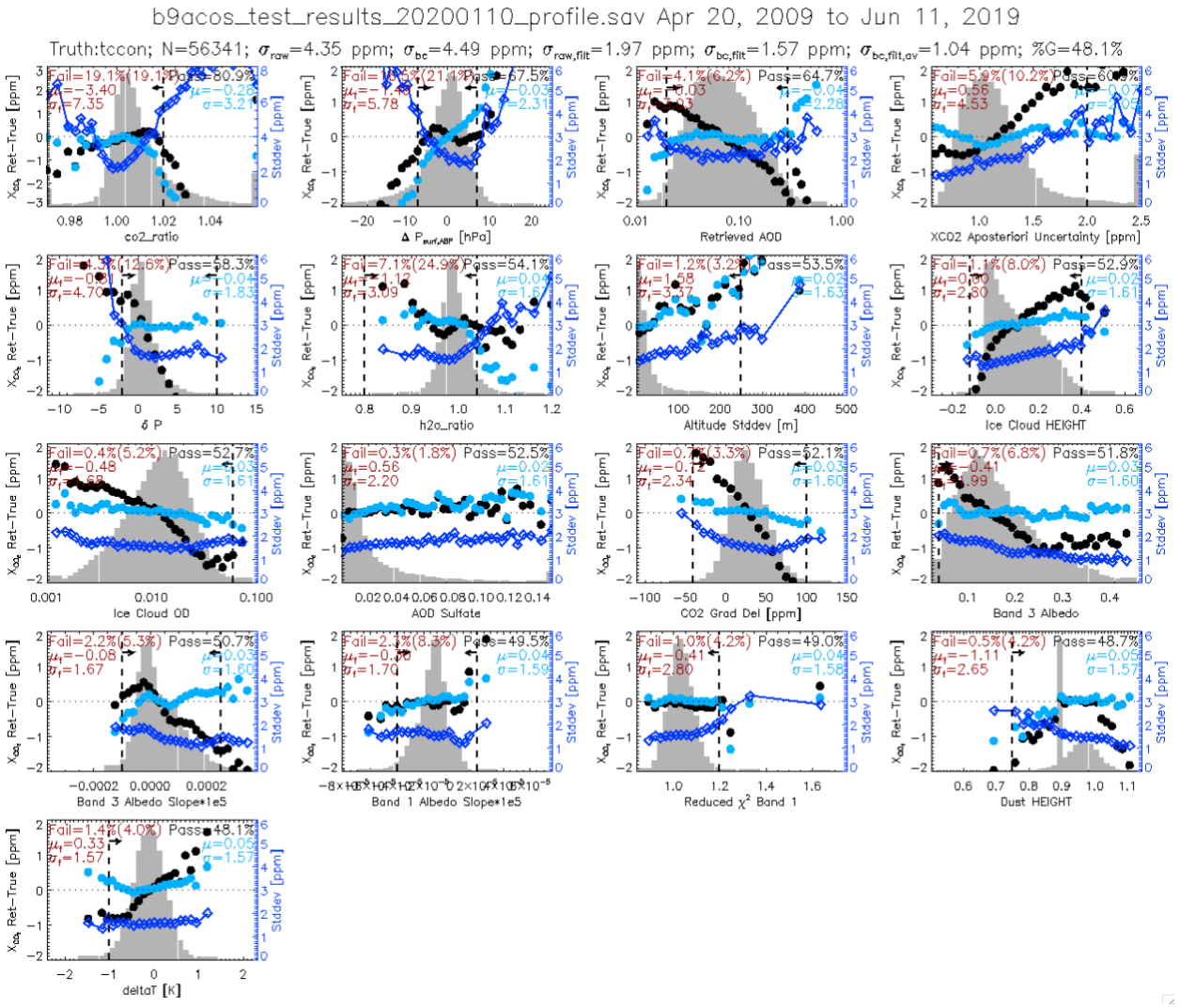

Figure 2: Plot showing the land gain H filtering process, without (black) and with (light blue) bias correction. Each panel shows the mean bias of the retrieved X_{CO2} as evaluated against TCCON for the v9 dataset. The figure should be read left-to-right, top-to-bottom. Each panel shows the effect of a filter variable, applied cumulatively to all the variables that came before it. In the top right corner of each panel is displayed the number of surviving soundings after that filter has been applied (again, cumulatively), and the standard deviation of the X_{CO2} errors for those soundings surviving to that point. The dark blue diamonds show the standard deviation of the X_{CO2} error in each bin.

2.5.5. Recommended Bias Correction

In addition to a global bias, errors in the X_{CO2} retrievals have been found to correlate well with certain other variables. This has been true in all previous versions of the algorithm. This issue was first explored for B2.8 and B2.9 (Wunch et al., 2011), in which four regression variables were used to correct ACOS (land, gain H) data. No correction was given for land gain M or ocean glint data at that time. This procedure was expanded in the B2.10 retrievals to also include land gain M and ocean glint soundings. There, two variables were used to bias-correct land soundings, and three were used for ocean soundings. The same methodology was followed in v3.3 for land gain H data only (as land gain M and ocean data were not trustworthy from this version), and a two-parameter bias-correction was found there. A similar procedure was followed for v3.4 for all 3 modes (land gain H, land gain M, ocean glint).

For v9 retrievals, we again follow the same methodology but again arrive at slightly different bias-correcting variables and coefficients as compared to previous versions. This is due to the changes in the algorithm, primarily due to the new aerosol treatment. For the bias correction formulae given below, there is some uncertainty in the fit coefficients as well as the overall mean bias. We estimate these uncertainties for each parameter and mean bias term, as rough 1-sigma uncertainties. These may be incorporated into inversion systems to formally account for these uncertainties. The uncertainties were obtained by using both models and TCCON as validation data sources, and the differences in the fit coefficients were used as a rough proxy for uncertainty.

The following bias correction formulae have been derived separately for land gain H, land gain M, and ocean glint. All formulae were derived using multiple linear regression to both TCCON, version ggg2014, and model data. Mean bias terms were estimated solely from TCCON (version ggg2014). Coefficient values and their parameters are given in Table 2. For the first time, with now ~10 years of data, a small time trend is also seen in the data, so this too is removed in the bias correction. The time trend is ~ -0.05 ppm/yr for retrievals over land, and ~ -0.10 ppm/yr for ocean glint retrievals.

2.5.6. V9 (first release) bias correction (recommended)

In units of ppm, the XCO2 bias correction formulae are as follows. "Year" means the full fractional year, e.g. 2015.0 means Jan 1, 2015 at 0.0 UTC.

Land Gain H

$$X_{CO2}' = X_{CO2} + 0.95 + 0.64\,(\mathrm{dPfrac}) + 4.6\,(\alpha_3 - 0.04) + 0.0236\,(\Delta Grad_{CO2} - 25) + 12.2\,(DWS - 0.02) + 0.05\,(\mathrm{Year} - 2015.0)$$

Land Gain M

$$X_{CO2}' = X_{CO2} + 0.50 + 0.705\,(\mathrm{dPfrac}) + 7.0\,(\sqrt{\alpha_3} - 0.2) + 0.0275\,(\Delta Grad_{CO2} - 50) + 7.6\,(\sqrt{DWS} - 0.25) + 0.05\,(\mathrm{Year} - 2015.0)$$

Ocean Glint

$$X_{CO2}' = X_{CO2} + 0.60 - 0.128\,(\Delta Grad_{CO2}) + 41.4\,(\max(\mathrm{eof3\_3}, 0.0)) + 0.10\,(\mathrm{Year} - 2015.0)$$

where α3 is the retrieved albedo in Band 3 (BRDFResults/brdf_reflectance_strong_co2_fph). logDust is the natural logarithm of the AOD_Dust (defined in the previous section). All other variables were defined in the preceding section.

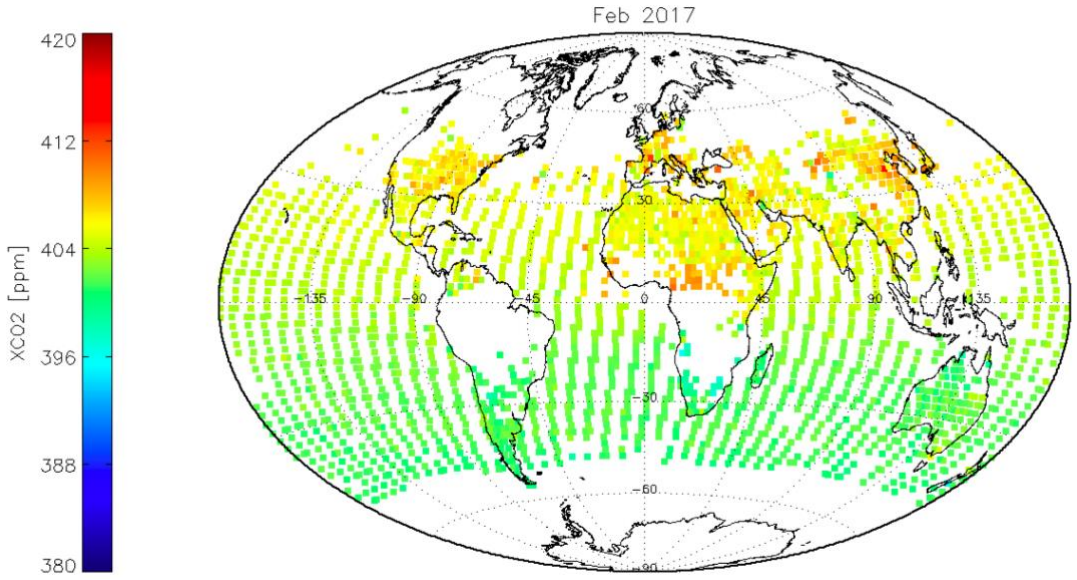

Figure 3: ACOS/GOSAT XCO2 data for February 2017 after screening.

Some users may wish to have information regarding the uncertainty in the bias correction. This is difficult to quantify for a number of reasons. First, the validation data source (such as TCCON or the SH Approximation as used in Wunch et al., 2011) each have their own uncertainties and limitations. Training the bias correction separately on each generally results in slightly different fit coefficients. Second, the ACOS soundings themselves have errors, and incorporating all these error sources into a robust parameterization of the bias correction error is nontrivial. Therefore, the uncertainties given in Table 2 are only rough estimates, based loosely on the above considerations.

Table 2: v9 bias correction parameters and their estimated uncertainties.

Bias Correction Parameters	Value ± Uncertainty (1σ)
Land Gain H	
d*Pfrac* Coefficient	-0.64 ± 0.05
α_3 Coefficient	-4.6 ± 1.0
$\Delta Grad_{CO2}$ Coefficient	-0.0236 ± 0.002
DWS Coefficient	-12.2 ± 1.5
Year Coefficient	-0.05 ± 0.02
Mean Bias [ppm]	-0.95 ± 0.25
Land Gain M	

dPfrac Coefficient	-0.705 ± 0.05
$\sqrt{\alpha_3}$ Coefficient	-7.0 ± 1.0
$\Delta Grad_{CO2}$ Coefficient	-0.0275 ± 0.002
$\sqrt{DWS}$ Coefficient	-7.6 ± 1.0
Year Coefficient	-0.05 ± 0.02
Mean Bias [ppm]	-0.50 ± 0.25
Ocean Glint	
$\Delta Grad_{CO2}$ Coefficient	0.128 ± 0.02
Max(eof3_3,0.0)	-41.4 ± 5.0
Year Coefficient	-0.10 ± 0.02
Mean Bias [ppm]	-0.60 ± 0.25

2.5.7. Model-data comparisons and application to flux inversions

When comparing the ACOS XCO_2 to models, it is recommended to make use of our column averaging kernel. The ACOS level-2 retrieval first retrieves a profile of CO_2 dry-air mole fraction on twenty layer boundaries. The lowest pressure boundary is at the surface. XCO_2 given as:

$$X_{CO2} = \boldsymbol{h} \times \boldsymbol{u} \tag{2.6}$$

where $\boldsymbol{h}$ is the pressure weighting function vector and $\boldsymbol{u}$ is the retrieved vector of CO_2 dry air mole fraction. In theory, we retrieve a weighted average of the true profile and our prior profile, plus a contribution from measurement noise:

$$\boldsymbol{u} = \boldsymbol{A}\boldsymbol{u}_{true} + \left(\boldsymbol{I} - \boldsymbol{A}\right)\boldsymbol{u}_{ap} + \boldsymbol{G}\boldsymbol{\varepsilon} \tag{2.7}$$

where $\boldsymbol{A}$ is the full averaging kernel matrix, $\boldsymbol{u}_{true}$ is the true profile of CO_2, $\boldsymbol{u}_{ap}$ is the prior profile of CO_2 used by the L2 code, $\boldsymbol{G}$ is the retrieval gain matrix, and $\boldsymbol{\varepsilon}$ is measurement noise. Hitting this equation with the pressure weighting function on the left, we arrive at a simple equation for our retrieved XCO_2:

$$X_{CO2} = \boldsymbol{a} \cdot \boldsymbol{u}_{true} + \left(\boldsymbol{h} - \boldsymbol{a}\right) \cdot \boldsymbol{u}_{ap} + \left(\boldsymbol{h}^t \boldsymbol{G}\right) \cdot \boldsymbol{\varepsilon} \tag{2.8}$$

where $\boldsymbol{a}$ is the called the (un-normalized) column averaging kernel. When comparing to models, it is useful to form the normalized column averaging kernel $\boldsymbol{a}_{\text{norm}}$, where

$$\boldsymbol{a}_{norm,i} = \boldsymbol{a}_i / \boldsymbol{h}_i \tag{2.9}$$

for each of our 20 levels i. When comparing model XCO_2 to measured, one should interpolate the model CO_2 profile to the ACOS pressure grid, and call that the truth in equation 2.8 (and setting the noise term to zero). $\boldsymbol{h}$ and $\boldsymbol{a}$ are both given in the data files. The vertical grid in the level-2 retrieval algorithm is a sigma pressure grid, such that the pressure at level i is given by

$$P_i = b_i P_{surf} \quad (2.9)$$

Here, P_{surf} is the retrieved surface pressure and b is vector of 20 coefficients (one for each vertical level). This is called "SigmaB" in the ACOS Lite product file. For versions after v3.4, this vector is ***b****=(1e-4, 1/19, 2/19, …18/19,1.0)*.

For users need the full state vector averaging kernel and/or covariances matrices, these are available upon request (please email Christopher.ODell@colostate.edu).

2.5.8. GOSAT H- and M-Gain Data

The TANSO-FTS on the GOSAT satellite makes measurements in different modes. The different gain modes appear to suffer from slightly different biases, and the bias correction described above attempts to correction for these differences. Therefore, users should recognize that these differences exist, and while there is a bias-correction, it is not perfect and it is important to recognize that there may be residual differences in XCO_2 errors between these modes.

The gain setting can be determined by looking at the "RetrievalHeader/gain_swir" variable in the ACOS data product. Note that this variable has two character string entries per sounding – one for the S polarization and one for the P polarization. For ACOS retrievals, P & S polarizations have been averaged together to produce an approximation of the total intensity I.

3. Background Reading

3.1. About the GOSAT Mission

The Japanese GOSAT mission was successfully launched on January 23, 2009. The GOSAT prime mission extends five years from the date it was declared operational on April 19, 2009 (Kuze et al., 2009).

3.1.1. Instrument

The primary GOSAT science instrument is the Thermal And Near infrared Sensor for carbon Observation (TANSO). It is a Fourier-Transform Spectrometer (FTS) with 2-axis scanner. The scanner directs light into two sets of detectors within the instrument, Figure 4.

The Short Wave InfraRed (SWIR) detector is designed to measure the spectrum of reflected sunlight from both land and water surfaces. Three spectral regions are covered in two polarizations:

Band 1	.75 - .78 µm	Oxygen, a.k.a. ABO2
Band 2	1.56 – 1.72 µm	Weak CO_2, a.k.a. WCO2
Band 3	1.92 – 2.08 µm	Strong CO_2, a.k.a. SCO2

The Thermal InfraRed (TIR) detector is designed to measure the spectrum of thermal radiation from both land and water surfaces. A single spectral region is covered (5.5 – 14.3 µm). The ACOS Level 2 products do not include or utilize any TIR data.

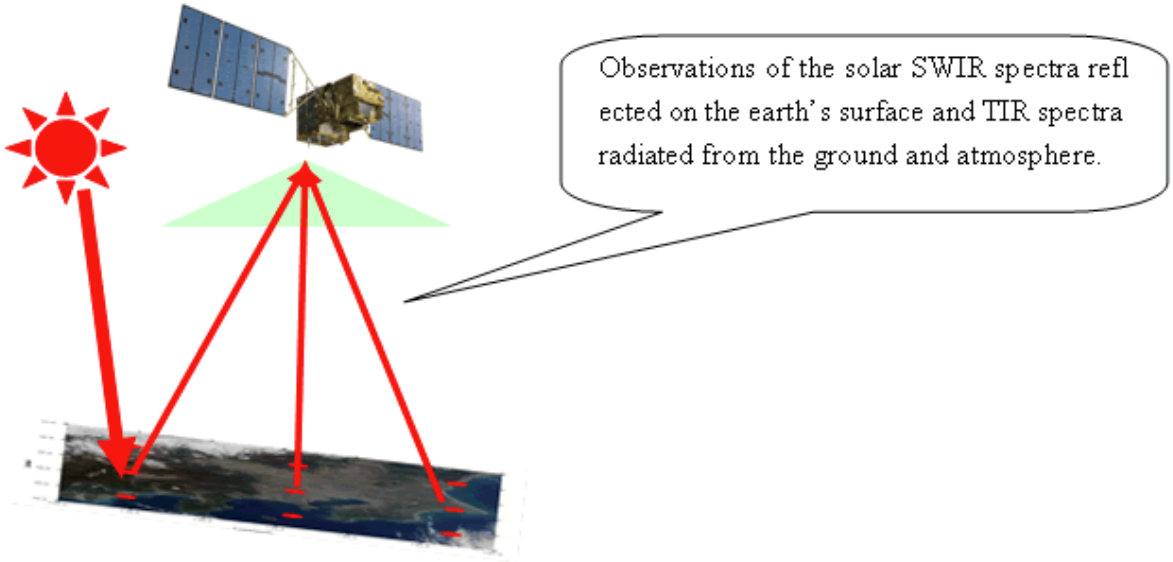

Figure 4: GOSAT Observation Concept.

3.1.2. Orbital Parameters

GOSAT nominal orbit parameters are shown below.

- Orbit Type: Sun-synchronous, ground track repeat, near-circular
- Recurrent period: 3 days
- Recurrent orbit number: 44
- Revolutions per day: 14+2/3 rev/day
- Local sun time at descending node: 12:45 – 13:15 PM
- Altitude above equator: 665.96 km
- Orbital Period: 98.1 minutes
- Inclination: 98.06 degrees
- Eccentricity: 0.0 (Frozen orbit)
- Longitude at ascending node: Longitude 4.92 degrees west for orbit 1
- Footprint size on ground 10.5 km circle when NADIR viewing

3.1.3. Path ID Definition

The Path ID identifies the GOSAT orbit tracks on the ground. The detailed characteristics are as follows:

A path begins at ascending node and extends to the next ascending node

The ascending node of the Path with an ID of 1 is at longitude 4.92 degrees west

The path number of the orbit tracks westward sequentially

Path IDs run from 1 through 44

Path calculator: https://data.gosat.nies.go.jp/map/html_E/MapPathCalendar.html

Note that Figure 5 illustrates 5-point sampling, which was used from April 2009 through July of 2010. Since August of 2010, a 3-point sampling mode has been used.

Points	Interval
1	789 km
3	263km
5 (nominal)	158km
7	113km
9	88km

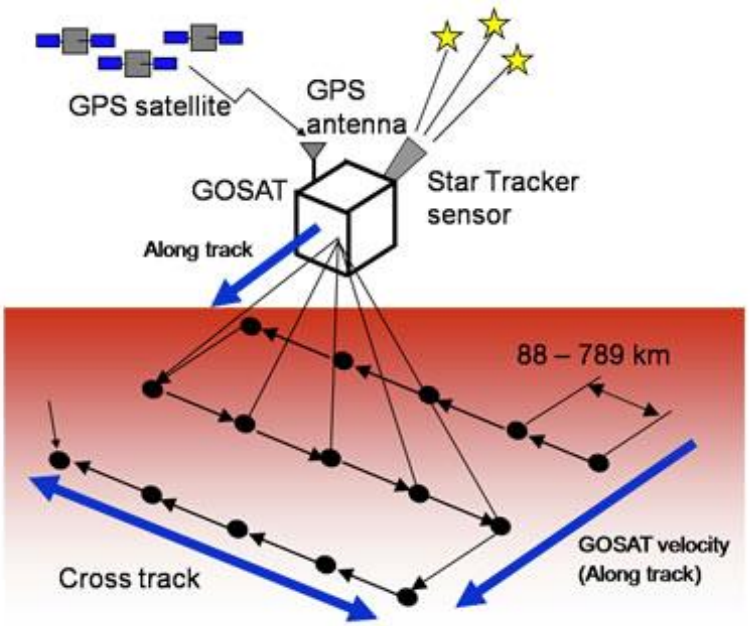

Figure 5: GOSAT TANSO-FTS Observation Details.

3.2. GOSAT L1B Releases

The L1B radiance data are provided to the ACOS project by JAXA. As instrument characteristics are better understood, there have been some changes to the L1B data. Table 3 provides a high level view of the L1B versions and key characteristics. Section 3.5.1 shows how the L1B version that was used can be identified in the L2 product file name.

3.3. About the ACOS Task

The ACOS project is part of the Earth System Science Pathfinder (ESSP) Program in the NASA Science Mission Directorate (SMD). The Orbiting Carbon Observatory (OCO) was to have been the first NASA satellite designed to make global measurements of atmospheric carbon dioxide (CO_2) sources and sinks on regional scales at monthly intervals. The failure of the launch system and loss of the observatory therefore represented a setback to NASA's carbon cycle and climate science programs.

To meet its stringent CO_2 measurement accuracy requirements, the OCO Science Team developed and implemented several significant advances in ground-based calibration, validation, and remote sensing retrieval methods. These investments were not lost in the OCO launch failure and remain valuable NASA assets.

The OCO and GOSAT Science Teams formed a close partnership in calibration and validation activities. JAXA granted the ACOS Project access to GOSAT's calibrated Level 1B measurements. The ACOS Project applies the OCO calibration, validation, and remote sensing retrieval assets to analyze these GOSAT measurements. These analyses generate the Level 2 data products described herein.

After the launch of OCO-2 and the Orbiting Carbon Observatory-3 (OCO-3), the OCO teams made a decision to do a full reprocessing of the ACOS/GOSAT data record to cover the 2009-2019 time period.

Table 3: Description of the different GOSAT L1B releases.

Version	Period YYMMDD	Changes
Version006006 (P)	090423–090504 090516–090728	• Initial version
Version007007 (P)	090405–090409 090419–090429 090716–091029	• SWIR spectrum unit is changed: (V -> V/cm-1) • SWIR phase correction parameter is changed. (Gauss function parameter; 0.060000 -> 0.002000, see "TANSO Level 1Product Description Document" page 3-29) • Orbital data is changed. (predicted value -> fixed value) • Threshold of sun-glint cone angle is changed. (10 degrees -> 5 degrees) • New product items are added.
Version050050	090405–090409 090419–090503 090602–090731 091028–100208	• TIR phase correction (ZPD shift) • New item on spike noise judgment is added. • Threshold of saturation flag is changed. • Low-frequency correction. flag judgment is improved.
Version080080	090731–091001 100208–100316	• Calibration formula of TIR radiance spectrum are added. (But parameters are modified so that radiance values remain the same as those for V050.) • The accuracy of SWIR spike flag judgment is improved. • "CT_obsPoints" value is changed to "0X0a", when sensor mode is "specific point observation". As a result, it can be distinguished from the case of sensor anomaly. • AT/CT error angles are expressed in GOSAT/TANSO sensor coordinate. • Orbit and attitude parameters are changed.
Version100100	090930–091031 100315–110419	• "The major updated point on Ver.100_100 is that TIR phase correction. There are no change in SWIR processing so there is no difference in SWIR spectrum between current Ver.080_080 and Ver.100_100." - e-mail from Akihiro Matsushima

Version	Period YYMMDD	Changes
Version130130	110419–120418	• Preliminary Band-1 analog circuit non-linearity correction, based on ADC non-linearity implemented. • Adjustment of saturation detection. • Modification to TIR calibration. • No v2.10 ACOS Level 2 data products produced with this version of GOSAT L1B
Version141141	090601-100731	• Modified correction to Band-1 analog circuit non-linearity • Correction to the interferogram sampling interval uniformity • Improvement of TIR phase correction • Improvement of the Band-1 scan speed instability correction for medium gain (Gain M) data. • Processed using the 32-bit Level-1 processing system • No v2.10 ACOS Level 2 data products produced with this version of GOSAT L1B
Version150150	120419-120619	• Identical to v141141, but processed on the 64-bit L1B production processing system
Version150151	090423 -091031* 101224 -111130* 120620-current	• Identical to v150150, but with a corrected glint flag. • *All L1B data will be reprocessed to this version by December 2012.
Version161160	090422 - 140607	• An optical path difference (OPD) sampling interval non-uniformity correction (SINUC) was applied in L1B V150. However, a spectral ringing artifact was inadvertently introduced to the spectra in the L1B V150 processing, as 100 zeros were filled in at both ends of the interferogram. The L1B V161 processing switched off SINUC to correct this mistake • An update to how the calibration of the TANSO FTS thermal infrared measurement in spectral band 4 is performed. V161 includes a more accurate polarization reflectance for each mirror.
Version 201201	090422 - 160331	• Bug Fix of unexpected values of some data-sets (ZPD_MissFlag, masterQualityFlag, ZPD_ShiftFlag, satelliteAttitudeStabilityFlag and attributes of dataset) and the condition of ZPD Bias Correction.
Version 205205, 210210	160401 – Current	• V205 (April 2009 to February 2018) • V210 (March 2018 to December 2019)

The GOSAT team at JAXA produces GOSAT TANSO-FTS Level 1B (L1B) data products for internal use and for distribution to collaborative partners, such as ESA and NASA. These calibrated products are augmented by the ACOS Project with additional geolocation information

and further corrections. These ACOS Level 1B products (with calibrated radiances and geolocation) are the input to the ACOS Level 2 production process.

The distribution of GOSAT and ACOS L1B products is currently restricted by cooperation agreements between JAXA and NASA.

3.4. ACOS Algorithms

In the sections that follow, the following definitions apply:

Footprint – an observation by a single instrument

Sounding – a combined observation of all instruments

Granule – the construct expressing the content of a product (ACOS product granules contain all the processed GOSAT data for a single orbit)

3.4.1. Level 1B Algorithm Overview

The ACOS Level 1B (L1B) algorithm adds additional calibration information to the GOSAT TANSO-FTS Level 1B data, and converts these data to the format needed for the ACOS Level 2 algorithm. For example, the TANSO-FTS L1B is delivered with radiances expressed in engineering units (volts). JAXA provides a series of calibration tables that are used to convert these values from engineering units to the radiometric units used in the ACOS algorithm (photons/m^2/sr/cm^{-1}). The calibration information provided in these tables is derived from pre-launch calibration tests and on-orbit observations of internal light sources, deep space, the sun, the moon, and observations of calibration targets on the surface of the Earth. These tabulated results are assumed to be constant, or used to establish trends for time-dependent corrections.

Sounding and spacecraft geometric variables are included in the ACOS Level 2 products. Starting with v2.9, these geometric data are updated by the ACOS team, based on pointing error estimates provided by the GOSAT Project Team. As noted above, the pointing error tables applied to v2.9 are based on observations collected prior to December 2010, and are assumed to be constant in time. Some aspect s of the geolocation' is performed by the ACOS team based on standard Earth geoid shape and a high-resolution digital elevation model (DEM) and some is copied from the GOSAT input products.

ACOS does not currently process all soundings collected by GOSAT. Because the thermal IR data is not utilized in ACOS, only the soundings in the daylight portion of the GOSAT orbit are processed. This version of processing supports both nadir and glint soundings. Details of glint soundings are provided in section 2.5.2.

In addition, to restrict the attempted retrievals to those with adequate signal, the soundings are also screened by the expression "*sounding_solar_zenith* < 85".

Performing retrievals on scenes containing clouds will either fail or have skewed results (depending upon the extent of cloud coverage). Users should check the *cloud_flag* for the ACOS estimate of scene cloudiness. Many cloudy scenes that are inadvertently passed by the cloud screen algorithm will not converge during the processing and, therefore, will not appear in the Level 2 retrieval results.

3.4.2. Level 2 Algorithm Overview

The Full-physics XCO_2 retrieval algorithm is based on the one that was to be used for the Orbiting Carbon Observatory (OCO). The algorithm is a Rodgers [2000]-type optimal

estimation approach and has been described fully in O'Dell *et al*. [2011]. The retrieval algorithm consists of a forward model, an inverse method, and an error analysis step. The overall flow for the retrieval process is shown in Figure 6.

The basic idea is to use a forward model to simulate all three bands of the OCO-2 spectrum then fitting the measured spectra to the model. The forward model contains components simulating the solar spectrum, atmospheric scattering and absorption, surface optical properties, radiative transfer, and detection by the instrument. The input to the forward model consists of meteorological conditions, surface properties, characteristics of the instrument, etc. Everything that is necessary to fully simulate the as-measured radiances must be input to the forward model.

The residuals between the simulated and measured spectra are minimized by changing parameters in the state vector via the inverse method. This inversion is relatively efficient because the forward model returns not just simulated radiances, but also partial derivatives of those radiances, also called Jacobians. The Jacobians are used by the inverse model to efficiently update the state vector in order to quickly find the state that minimizes the residuals.

Once the atmospheric state yielding the best match to the observed spectrum has been found, the algorithm then determines X_{CO2}, errors in X_{CO2} from different sources (such as vertical smoothing, measurement noise, etc.), and the X_{CO2} column averaging kernel. This is necessary because *xco2* is not itself an element of the state vector. Rather, it is determined from the profile of CO_2, which is part of the state vector. It is formally given by the total number of CO_2 molecules in the column divided by the total number of dry air molecules in the column. This step is labeled "Error Analysis" in Figure 6.

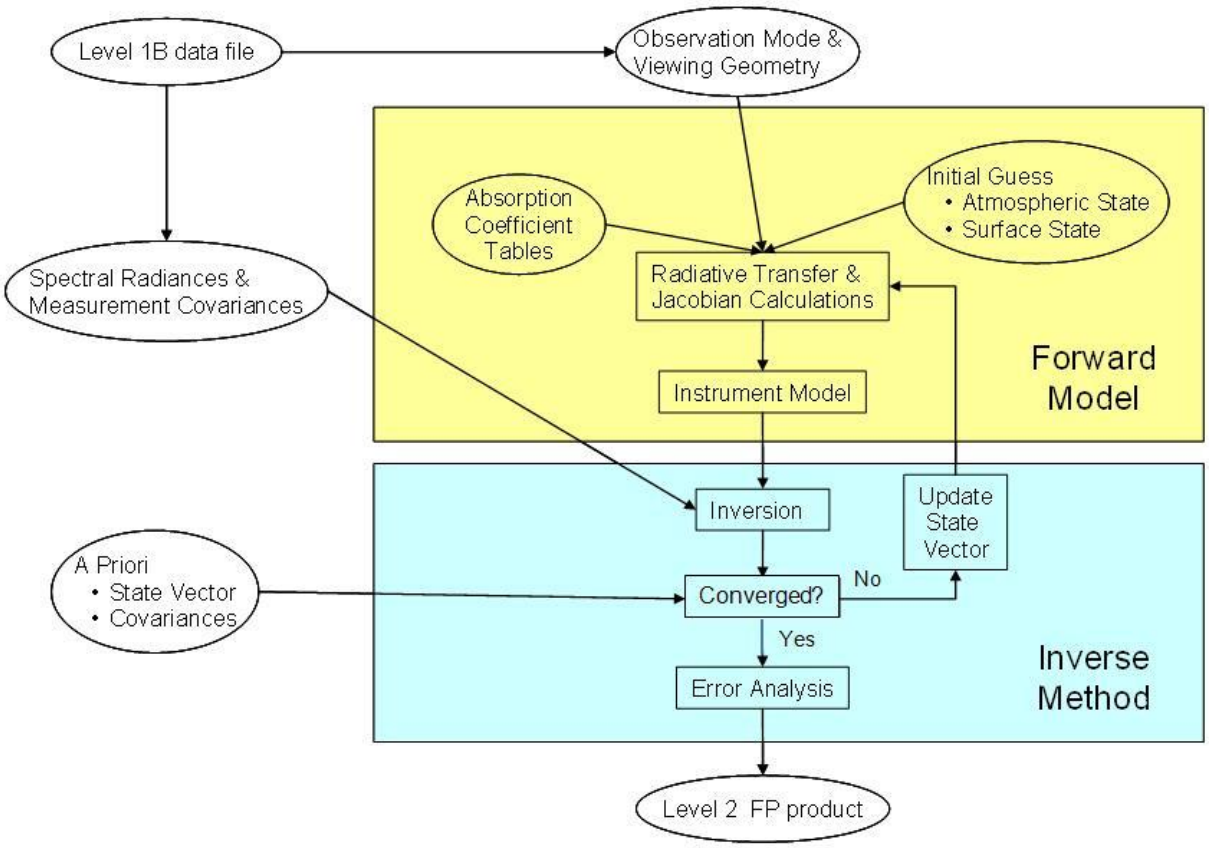

Figure 6: Level 2 Full Physics Retrieval Flow

3.5. ACOS Data Products – L2 Standard Data

The ACOS Level 2 product set consists of products that focus on measuring column-averaged CO_2 dry air mole fraction (X_{CO_2}). The measurements are extracted from observations made by JAXA's Greenhouse gases Observing SATellite (GOSAT). The global coverage that is achieved by GOSAT is repeated every three days at the highest resolution yet achieved from orbit.

3.5.1. File Naming Convention

ACOS Level 2 Product file name specification:
acos_ttt_date_nn_collection_productionTimeStamp**.h5**

Where:

ttt = product type (L2s)

date = observation date (yymmdd)

nn = GOSAT path number (01-44)

collection = B[xxxx] which is the label for L2 retrieval version

Pol[x] = the polarization used for the retrievals; possible values are S, P, or B (both)
productionTimeStamp = production date/time (UTC) at ACOS (yymmddhhmmss)

Filename examples:

acos_L2s_190822_22_B9200_PolB_200309225616.h5

acos_L2s_150214_19_B9200_PolB_190811065100.h5

3.5.2. File Format and Structure

All ACOS Level 2 product files are in HDF-5 format, developed at the National Center for Supercomputing Applications http://www.hdfgroup.org/. This format facilitates the creation of logical data structures.

All ACOS Level 2 product files contain data structures indexed by sounding (1 to N soundings/file) and are associated by the *sounding_id* variable in all products.

Variables are combined into groups by type (e.g., SoundingGeometry). Within each type, a variable has one or more values per sounding. Variables may be single-valued (e.g., *sounding_altitude*) or multi-valued (e.g., *co2_profile*).

The metadata of each variable describes the variable's attributes, such as dimensions, data representation and units.

3.5.3. Data Definition

The ACOS Level 2 products contain many variables with a variety of dimensions. The following list describes only the most important of the dimensions.

- Retrieval: The number of retrievals reported (those soundings for which
- Polarization: The number of polarization states
- Level: The number of atmospheric retrieval levels
- Exposure: The number of scans in granule
- Band: The number of spectral bands
- Aerosol: The number of retrieval aerosol types

3.5.4. Global Attributes

In addition to variables and arrays of variables, global metadata is stored in the files. Some metadata are required by standard conventions, some are present to meet data provenance requirements and others as a convenience to users of the ACOS Level 2 Products. The most useful global attributes present in all files are shown in Table 4. Table 5 provides a list of key metadata fields for each variable.

Table 4: Some Global Metadata Attributes

Global Attribute	Type	Description
AscendingNodeCrossingDate	String	The date of the ascending node crossing immediately before the first exposure in the TANSO-FTS file. Format: yyyy-mm-dd
AscendingNodeCrossingTime	String	The time of the ascending node crossing immediately before the first exposure in the TANSO-FTS file. Format: hh:mm:ss.sssZ
StartPathNumber	32-bit integer	The first orbital path on which data contained in the product was collected.
StopPathNumber	32-bit integer	The last orbital path on which data contained in the product was collected.
ProductionDateTime	String	The date and time at which the product was created.
CollectionLabel	String	Label associating files in a collection.
HDFVersionId	String	For example 'HDF5 1.8.5'. A character string that identifies the version of the HDF (Hierarchical Data Format) software that was used to generate this data file.
BuildId	String	The identifier of the build containing the software that created the product.
TFTSVersion	String	The version of the TANSO FTS data used to create this data product.

Table 5: Key Metadata Fields

Name	Type	Description
Name	String	The name of the variable
Shape	String	The set of dimensions defining the structure
Type	String	The data representation type
Description	String	The units of the variable.

3.5.5. ACOS L2 Standard Data Tables and Fields

This section contains tables describing the groups of variables and data elements for the ACOS L2 Standard product.

Table 6 provides information on ACOS metadata.

Table 6: Metadata Information

Element	Storage	Comment
AbscoCO2Scale	Float32	Empirical scaling factors for CO2 ABSCO tables. Values should be different for the 1.6 micron and 2.06 micron bands and were chosen to provide agreement of retrieved XCO2 with TCCON XCO2.
AbscoH2OScale	Float32	Empirical scaling factor for H2O ABSCO tables. Currently should be 1.0.

Element	Storage	Comment
AbscoO2Scale	Float32	Empirical scaling factor for O2 ABSCO tables. Values chosen to improve agreement between retrieved surface pressure and independent estimates from a numerical weather prediction model.
AncillaryDataDescriptors	String	An array of file names that specifies all of the ancillary data files that were used to generate this output product. Ancillary data sets include all input except for the primary input files.
AscendingNodeCrossingDate	String	The date of the ascending node crossing immediately before the first exposure in the TANSO-FTS file. Format: yyyy-mm-dd
AscendingNodeCrossingTime	String	The time of the ascending node crossing immediately before the first exposure in the TANSO-FTS file. Format: hh:mm:ss.sssZ
AutomaticQualityFlag	String	Reserved for future use.
BuildId	String	The identifier of the build containing the software that created the product.
CollectionLabel	String	Label associating files in a collection
DataFormatType	String	'NCSA HDF' - A character string that describes the internal format of the data product.
FirstSoundingId		The *sounding_id* of the first sounding in the file
GranulePointer	String	The name of the product.
HDFVersionId	String	'HDF5 vvvvvv' - A character string that identifies the version of the HDF (Hierarchical Data Format) software that was used to generate this data file where vvvvvv is a version id.
InputPointer	String	The name of the data product that provides the major input that was used to generate this product.
InstrumentShortName	String	'TANSO-FTS' - The name of the instrument that collected the telemetry data.
L2FullPhysicsAlgorithmDescriptor	String	A short description of the Full-Physics algorithm that was used to generate this product
L2FullPhysicsDataVersion	String	Indicates the build version number of the Full-physics algorithm used.
L2FullPhysicsExeVersion	String	Indicates the build version number of the Full-physics algorithm used.
L2FullPhysicsInputPointer	String	List of the input files used by the Full-physics algorithm code
L2FullPhysicsProductionLocation	String	
LastSoundingId	Int64	The *sounding_id* of the last sounding in the file
LongName	String	A complete descriptive name for the product.
MissingExposures	Int32	Number of expected points missing from the dataset
NominalDay	String	The approximate date on which the data were acquired. A *NominalDay* starts at an orbit boundary, so the *NominalDay* for some data do not match their calendar day. Format: yymmdd
NumberOfExposures	Int32	Actual number of points reported in the product

Element	Storage	Comment
NumberOfGoodRetrievals	Int32	Number of retrievals with master_quality_flag of Good
OrbitOfDay	Int8	The ordinal number of the orbit within its *NominalDay*, starting with 1.
PlatformLongName	String	'Greenhouse gases Observing SATellite'
PlatformShortName	String	'GOSAT'
PlatformType	String	'spacecraft' - The type of platform associated with the instrument which acquires the accompanying data
ProcessingLevel	String	Indicates processing level. The allowed values are: Level 1A, Level 1B, Level 2
ProducerAgency	String	'NASA' - Identification of the agency that provides the project funding
ProducerInstitution	String	'JPL' - Identification of the institution that provides project management.
ProductionDateTime	String	The date and time at which the product was created.
ProductionLocation	String	Facility in which the file was produced: "Operations Pipeline", "Test Pipeline", "SCF", "Preflight Instrument Characterization", "Development", "Orbital", "Unknown"
ProductionLocationCode	String	One-letter code indicating the *ProductionLocation*. The allowed values are: "" (null string) - Operations Pipeline s - SCF t - Test Pipeline c - Preflight Instrument Characterization d - Development o - Orbital x - Unknown
ProjectId	String	'ACOS' - The project identification string.
QAGranulePointer	String	A pointer to the quality assurance product that was generated with this product.
RangeBeginningDate	String	The date on which the earliest data contained in the product were acquired. Format: yyyy-mm-dd
RangeBeginningTime	String	The time at which the earliest data contained in the product were acquired. Format: hh:mm:ss.sssZ
RangeEndingDate	String	The date on which the latest data contained in the product were acquired. Format: yyyy-mm-dd
RangeEndingTime	String	The time at which the latest data contained in the product were acquired.
RetrievalIterationLimit	Int32	Maximum number of iterations allowed in the implementation of the retrieval algorithm

Element	Storage	Comment
RetrievalPolarization	String	Polarization used in TANSO-FTS measurements in this granule - "P", "S", or "B" (for Both).
ShortName	String	The short name used to identify all data granules in a given data collection.
SISName	String	The name of the document describing the contents of the product.
SISVersion	String	The version of the document describing the contents of the product.
SizeMBECSDataGranule	Float32	The size of this data granule in Megabytes.
SpectralChannel	String	The identifier of the spectral regions present in this granule. Allowed values are: '0.76um O2 A-band', '1.6um Weak CO2', '2.06um Strong CO2'
StartPathNumber	Int32	The first orbital path on which data contained in the product was collected.
StopPathNumber	Int32	The last orbital path on which data contained in the product was collected.
TFTSVersion	String	The version of the TANSO FTS data used to create this data product.
VMRO2	Float32	The Volume Mixing Ratio of atmospheric O2 in units of Mole Mole^{-1}

Table 7 describes variables related to the position of the spacecraft at the observation time. Note the variables have a Shape of 'Retrieval_Array'. Therefore, soundings are included only when retrievals converged or were converging when the maximum number of iterations was reached.

Table 7: Spacecraft Geometry Variables (Spacecraft Geometry)

Element	Type	Comment
ground_track	Float32	Azimuth of the spacecraft ground track (measured from North)
relative_velocity	Float32	The component of the relative SC/Target motion along the look-vector.
spacecraft_alt	Float32	Altitude of the spacecraft above the reference ellipsoid at the start of the exposure.
spacecraft_lat	Float32	Geodetic latitude of sub-spacecraft point at the start of the exposure.
spacecraft_lon	Float32	Longitude of sub-spacecraft point at the start of the exposure.
x_pos	Float32	Spacecraft position in Earth Centered Rotating (ECR) coordinates at the start of the exposure.
x_vel	Float32	Spacecraft velocity in Earth Centered Rotating (ECR) coordinates at the start of the exposure.
y_pos	Float32	Spacecraft position in Earth Centered Rotating (ECR) coordinates at the start of the exposure.
y_vel	Float32	Spacecraft velocity in Earth Centered Rotating (ECR) coordinates at the start of the exposure.

Element	Type	Comment
z_pos	Float32	Spacecraft position in Earth Centered Rotating (ECR) coordinates at the start of the exposure.
z_vel	Float32	Spacecraft velocity in Earth Centered Rotating (ECR) coordinates at the start of the exposure.

Table 8 describes variables related to the instrument look vector or the intersection of the look vector with the Earth surface. Note that the variables have a Shape of 'Retrieval_Array'. Therefore, soundings are included only when retrievals converged or were converging when the maximum number of iterations was reached.

Table 8: Sounding Geometry Variables (SoundingGeometry)

Element	Type	Comment
sounding_altitude	Float32	Mean altitude of the surface within the sounding based on PGS Toolkit topography
sounding_altitude_max	Float32	Maximum altitude of the surface within the sounding based on PGS Toolkit topography
sounding_altitude_min	Float32	Minimum altitude of the surface within the sounding based on PGS Toolkit topography
sounding_altitude_stddev	Float32	Standard deviation of the measure of altitude of the surface within the sounding
sounding_altitude_uncert	Float32	Uncertainty of the measure of altitude of the surface within the sounding based on the accuracy of the input information
sounding_aspect	Float32	Azimuth of the surface projection of the slope surface normal
sounding_at_angle	Float32	Angle between the look vector and the spacecraft Y-Z plane. Positive angle is the right-hand screw direction of the Y-axis.
sounding_at_angle_error	Float32	The difference between AT value derived by MMO and actual one is stored
sounding_azimuth	Float32	Azimuth of the vector toward the instantaneous position of the spacecraft from the center of the sounding based on topography
sounding_ct_angle	Float32	Angle between look vector and the spacecraft X-Z plane. Positive angle direction is the right-hand screw direction of the X-axis
sounding_ct_angle_error	Float32	The difference between CT value derived by MMO and actual one is stored
sounding_glint_angle	Float32	The angle between the vector to the glint spot and the actual look vector.
sounding_land_fraction	Float32	Percent of land cover within the sounding.
sounding_latitude	Float32	Geodetic latitude of the center of the sounding based on PGS Toolkit topography
sounding_latitude_geoid	Float32	Geodetic latitude of the center of the sounding based on standard geoid
sounding_longitude	Float32	Longitude of the center of the sounding based on PGS Toolkit topography
sounding_longitude_geoid	Float32	Longitude of the center of the sounding based on standard geoid
sounding_plane_fit_quality	Float32	Standard deviation for the tangent plane approximation

Element	Type	Comment
sounding_slope	Float32	Slope of the best-fit plane to the surface within the sounding.
sounding_solar_azimuth	Float32	Azimuth of the sun at the center of the sounding based on topography
sounding_solar_zenith	Float32	Angle between the normal to the Earth geoid and the solar angle at the center of the sounding based on topography
sounding_zenith	Float32	The angle between the normal to the Earth geoid and the vector toward the instantaneous position of the spacecraft from the center of the sounding based on topography

Table 9 describes Sounding Header fields. They all have the Shape 'Exposure_Array" and, therefore, include all soundings.

Table 9: Sounding Header Variables (SoundingHeader)

Element	Type	Comment
cloud_flag	Int8	Estimate of scene visibility for this *sounding_id* taken from an ABO2-only clear sky retrieval: 0 - Clear, 1 - Cloudy, 2 - Undetermined
l2_packaging_qual_flag	BitField8	Bit Flags are used to record the status of each sounding during packaging of l2 output into retrieval arrays. See Table 16.
retrieval_index	Int32	Index into the Retrieval dimension of arrays in the RetrievalResults group for soundings associated with retrievals.
sounding_id	Int64	The unique identifier of the sounding.

Table 10 describes data products related to cloud screening.

To further reduce the computation time of retrievals containing clouds, a cloud screening algorithm is applied to this version. It performs a fast, Oxygen A-band only clear-sky retrieval for surface pressure, surface albedo, temperature offset and dispersion multiplier. The retrieved surface pressure and albedo information are combined with the χ^2 goodness-of-fit statistic and signal-to-noise ratio to determine if a scene is clear (0), cloudy (1), or undetermined (2) as shown in Table 10. See Section 6 for a paper on this topic.

Table 10: A-Band-only Retrieval Variables (ABandCloudScreen)

Element	Type	Comment
albedo_o2_cld	Float32	Retrieved value of lambertian surface albedo at 785 and 755 nm, respectively; from the O2 A Band cloud retrieval.
dispersion_multiplier_cld	Float64	The retrieved wavenumber multiplier to get the best fit to the O2 A band; from the A Band cloud retrieval.
noise_o2_cld	Float32	The noise level in the O2 A band for (P+S)/2, averaged over the spectral samples with the ten highest radiance levels.
reduced_chi_squared_o2_cld	Float32	The reduced chi^2 value of the O2 A-band clear-sky fit used in determine the presence or absence of cloud; from the O2 A Band cloud retrieval.

Element	Type	Comment
reduced_chi_squared_o2_threshold_cld	Float32	The threshold of reduced_chisquared_o2_cld above which cloud_flag is set to 1.
signal_o2_cld	Float32	The signal level in the O2 A band for (P+S)/2, averaged over the spectral samples with the ten highest radiance levels.
snr_o2_cld	Float32	The value of the signal-to-noise ratio of (P+S)/2, averaged over the spectral samples with the ten highest radiance levels.
surface_pressure_apriori_cld	Float32	The value of the surface pressure of the center of GOSAT's field-of-view estimated from ECMWF; from the O2 A Band cloud retrieval.
surface_pressure_cld	Float32	The retrieved value of the surface pressure; from the O2 A Band cloud retrieval.
surface_pressure_delta_cld	Float32	surface_pressure_cld - surface_pressure_apriori_cld - surface_pressure_offset_cld
surface_pressure_offset_cld	Float32	The assumed surface pressure offset for clear-sky soundings, caculated from an empirical relation based on solar zenith angle, land/water and H/M gain; from the O2 A Band cloud retrieval.
temperature_offset_cld	Float32	The retrieved offset to the assumed profile of temperature taken from the prior (ECMWF) meteorology; from the O2 A Band cloud retrieval.

The IMAP-DOAS fields are listed in Table 11.

Table 11: IMAP-DOAS Retrieval Variables (IMAPDOASPreprocessing)

Element	Type	Comment
ch4_column_apriori_idp	Float32	A priori vertical column density of CH4 (climatology)
ch4_column_idp	Float32	Vertical column density of CH4 (weak band)
ch4_column_uncert_idp	Float32	1-sigma error in the vertical column density of CH4
ch4_weak_band_processing_flag_idp	Int8	0=processed, 1=failed, 2=not processed
cloud_flag_idp	Int8	Cloud&Aerosol filter flag; -2=unusable (outside of SZA range); -1=not all retrievals converged; 0=clearly cloudy; 1=probably cloudy; 2=probably clear; 3=very clear
co2_column_apriori_idp	Float32	A priori vertical column density of CO2 (climatology)
co2_column_ch4_window_idp	Float32	Vertical column density of CO2 retrieved in the CH4 fit window (very weak lines)
co2_column_strong_band_idp	Float32	Vertical column density of CO2 (strong band)
co2_column_strong_band_uncert_idp	Float32	1-sigma error in the vertical column density of CO2 (strong band)
co2_column_weak_band_idp	Float32	Vertical column density of CO2 (weak band)
co2_column_weak_band_uncert_idp	Float32	1-sigma error in the vertical column density of CO2
co2_ratio_idp	Float32	Ratio of retrieved CO2 column (no scattering code) in weak and strong CO2 ban
co2_strong_band_processing_flag_idp	Int8	0=processed, 1=failed, 2=not processed
co2_weak_band_processing_flag_idp	Int8	0=processed, 1=failed, 2=not processed
delta_d_idp	Float32	Deuterium depletion of total column water vapor
delta_d_uncert_idp	Float32	1-sigma uncertainty in deuterium depletion of total column water vapor

Element	Type	Comment
dry_air_column_apriori_idp	Float32	Integrated vertical column of dry airmass derived from meteorological data
h2o_column_apriori_idp	Float32	A priori vertical column density of H2O (based on ECMWF)
h2o_column_idp	Float32	Vertical column density of H2O
h2o_column_uncert_idp	Float32	1-sigma error in the vertical column density of H2O
h2o_ratio_idp	Float32	Ratio of retrieved H2O column (no scattering code) in weak and strong CO2 band
h2o_ratio_uncert_idp	Float32	1-sigma uncertainty in the ratio of retrieved H2O column (no scattering code) in weak and strong CO2 band
hdo_column_apriori_idp	Float32	A priori vertical column density of HDO
hdo_column_idp	Float32	Vertical column density of HDO
hdo_column_uncert_idp	Float32	1-sigma error in the vertical column density of HDO
hdo_h2o_processing_flag_idp	Int8	0=processed, 1=failed, 2=not processed
o2_ratio_p_idp	Float32	Ratio of retrieved and ECMWF O2 column retrieved in P-polarization
o2_ratio_s_idp	Float32	Ratio of retrieved and ECMWF O2 column retrieved in S-polarization
out_of_band_transmission_p_idp	Float32	Transmission at the band-pass edge, P-polarization, band 1
out_of_band_transmission_s_idp	Float32	Transmission at the band-pass edge, S-polarization, band 1
total_offset_fit_relative_755nm_p_idp	Float32	Total offset fit (0-level + fluorescence) as fraction of continuum level (755nm, P polarization)
total_offset_fit_relative_755nm_s_idp	Float32	Total offset fit (0-level + fluorescence) as fraction of continuum level (755nm, S polarization)
total_offset_fit_relative_771nm_p_idp	Float32	Total offset fit (0-level + fluorescence) as fraction of continuum level (771nm, P polarization)
total_offset_fit_relative_771nm_s_idp	Float32	Total offset fit (0-level + fluorescence) as fraction of continuum level (771nm, S polarization)

Table 12 describes the Retrieval Header, providing general characteristics of the soundings retrieved. Soundings are included only when retrievals converged or were converging when the maximum number of iterations was reached.

Table 12: Retrieval Header Variables (RetrievalHeader)

Element	Type	Comment
acquisition_mode	String	The instrument mode in which the data in the product were collected. Valid values are: 'OB1D', 'OB1N', 'OB2D','SPOD','SPON','CALM','LUCA'
ct_observation_points	Int8	Number of observation points in the cross track direction -1: undefined or specified observation, 0: Electrical Calibration, "0x01" : 1 points "0x03" : 3 points "0x05" : 5 points "0x07" : 7 points "0x09" : 9 points
dispersion_offset_shift	Float32	Spectral shifts estimated for this sounding from solar line at 12985.183 wavenmbers
exposure_duration	Float32	The duration of the exposure
exposure_index	Int32	The index into the Exposure dimension of arrays in SoundingHeader, SoundingGeometry, and

Element	Type	Comment
		SpacecraftGeometry groups containing the spectra used to perform the retrieval
gain_swir	String	Instrument gain setting for each polarization: H - High gain, M - Medium gain, L - Low gain, H_ERR - Error in setting high gain, M_ERR - Error in setting medium gain, L_ERR - Error in setting low gain, UNDEF - Gain set to an undefined state
glint_flag	Int8	This field is incorrect after YYYY-MM-DD. Use the glint filter described in section XXX instead of the glint_flag. Indicates whether GOSAT was in glint mode when acquiring the sounding 0 = Not in glint mode 1 = In glint mode
sounding_id_reference	Int64	The sounding_id of the sounding containing the spectra used to perform the retrieval
sounding_qual_flag	BitFlag32	Single-bit quality flags. See Table 16.
sounding_time_string	String	Representative sounding time, in the format yyyy-mm-ddThh:mm:ss.sssZ
sounding_time_tai93	Float64	Sounding time in number of SI seconds since midnight, January 1, 1993.
spike_noise_flag	Int8	0 - No spike noise present, 1 - Spike noise present
zpd_saturation_flag	Int8	Copy exposureAttribute/pointAttribute/RadiometricCorrectionInfo/ ZPD_SatiratopmFlag_SWIR

Table 13 describes variables expressing the retrieval results. Note that some of the variables have a Shape including 'Retrieval'. Therefore, soundings are included only when retrievals converged or were converging when the maximum number of iterations was reached.

In Table 13, *xco2* is calculated in the following way:

$$xco2 = \sum_{i=1}^{N_{num\_levels}} W_i CO2_i$$

where W_i represents *xco2_pressure_weighting_function* and $CO2_i$ represents *co2_profile*. The sum is over *num_levels*. W_i is a function primarily of the pressure level spacing, but also weakly of water vapor, and also depends on surface pressure.

Table 13: Variables Expressing Retrieval Results (RetrievalResults)

Element	Type	Comment
apriori_o2_column	Float32	Apriori vertical column of O2
co2_profile	Float32	Vertical profile of CO_2
co2_profile_apriori	Float32	Vertical apriori profile of CO_2
co2_profile_averaging_kernel_matrix	Float32	Averaging kernel for co2 profile
co2_profile_covariance_matrix	Float32	Covariance matrix for co2 profile

Element	Type	Comment
co2_profile_uncert	Float32	Vertical profile of CO_2 uncertainty
co2_vertical_gradient_delta	Float32	The change from apriori to retrieved value of the vertical gradient in the co2 profile. Indicates that the apriori co2 profile was substantially different than that which was retrieved.
diverging_steps	Int16	Number of iterations in which solution diverged
dof_co2_profile	Float32	Degrees of freedom (target gas profile only)
dof_full_vector	Float32	Degrees of freedom (Full state vector)
eof_1_scale_apriori_o2	Float32	A priori of retrieved scale factor of first empirical orthogonal residual function in ABO2 band
eof_1_scale_apriori_strong_co2	Float32	A priori of retrieved scale factor of first empirical orthogonal residual function in SCO2 band
eof_1_scale_apriori_weak_co2	Float32	A priori of retrieved scale factor of first empirical orthogonal residual function in WCO2 band
eof_1_scale_o2	Float32	Retrieved scale factor of first empirical orthogonal residual function in ABO2 band
eof_1_scale_strong_co2	Float32	Retrieved scale factor of first empirical orthogonal residual function in SCO2 band
eof_1_scale_uncert_o2	Float32	Uncertaintly of retrieved scale factor of first empirical orthogonal residual function in ABO2 band
eof_1_scale_uncert_strong_co2	Float32	Uncertaintly of retrieved scale factor of first empirical orthogonal residual function in SCO2 band
eof_1_scale_uncert_weak_co2	Float32	Uncertaintly of retrieved scale factor of first empirical orthogonal residual function in WCO2 band
eof_1_scale_weak_co2	Float32	Retrieved scale factor of first empirical orthogonal residual function in WCO2 band
eof_2_scale_apriori_o2	Float32	A priori of retrieved scale factor of second empirical orthogonal residual function in ABO2 band
eof_2_scale_apriori_strong_co2	Float32	A priori of retrieved scale factor of second empirical orthogonal residual function in SCO2 band
eof_2_scale_apriori_weak_co2	Float32	A priori of retrieved scale factor of second empirical orthogonal residual function in WCO2 band
eof_2_scale_o2	Float32	Retrieved scale factor of second empirical orthogonal residual function in ABO2 band
eof_2_scale_strong_co2	Float32	Retrieved scale factor of second empirical orthogonal residual function in SCO2 band
eof_2_scale_uncert_o2	Float32	Uncertaintly of retrieved scale factor of second empirical orthogonal residual function in ABO2 band
eof_2_scale_uncert_strong_co2	Float32	Uncertaintly of retrieved scale factor of second empirical orthogonal residual function in SCO2 band
eof_2_scale_uncert_weak_co2	Float32	Uncertaintly of retrieved scale factor of second empirical orthogonal residual function in WCO2 band
eof_2_scale_weak_co2	Float32	Retrieved scale factor of second empirical orthogonal residual function in WCO2 band
eof_3_scale_apriori_o2	Float32	A priori of retrieved scale factor of third empirical orthogonal residual function in ABO2 band
eof_3_scale_apriori_strong_co2	Float32	A priori of retrieved scale factor of third empirical orthogonal residual function in SCO2 band
eof_3_scale_apriori_weak_co2	Float32	A priori of retrieved scale factor of third empirical orthogonal residual function in WCO2 band

Element	Type	Comment
eof_3_scale_o2	Float32	Retrieved scale factor of third empirical orthogonal residual function in ABO2 band
eof_3_scale_strong_co2	Float32	Retrieved scale factor of third empirical orthogonal residual function in SCO2 band
eof_3_scale_uncert_o2	Float32	Uncertaintly of retrieved scale factor of third empirical orthogonal residual function in ABO2 band
eof_3_scale_uncert_strong_co2	Float32	Uncertaintly of retrieved scale factor of third empirical orthogonal residual function in SCO2 band
eof_3_scale_uncert_weak_co2	Float32	Uncertaintly of retrieved scale factor of third empirical orthogonal residual function in WCO2 band
eof_3_scale_weak_co2	Float32	Retrieved scale factor of third empirical orthogonal residual function in WCO2 band
fluorescence_at_reference	Float32	Retrieved fluorescence at 0.755 microns
fluorescence_at_reference_apriori	Float32	Apriori of retrieved fluorescence at 0.755 microns
fluorescence_at_reference_uncert	Float32	Uncertainty of retrieved fluorescence at 0.755 microns
fluorescence_slope	Float32	Retrieved fluorescence slope at 0.755 microns
fluorescence_slope_apriori	Float32	Apriori of retrieved fluorescence slope at 0.755 microns
fluorescence_slope_uncert	Float32	Uncertainty of retrieved fluorescence slope at 0.755 microns
h2o_scale_factor	Float32	Retrieved scale factor for h2o profile
h2o_scale_factor_apriori	Float32	Apriori of retrieved scale factor for h2o profile
h2o_scale_factor_uncert	Float32	Uncertainty of retrieved scale factor for h2o profile
iterations	Int16	Number of iterations
last_step_levenberg_marquardt_parameter	Float32	Levenberg Marquardt parameter corresponding to last iteration
num_active_levels	Int16	Number of levels in atmospheric model
outcome_flag	Int8	-2 = bad fill, -1 = packaging failure, 1 = passed internal quality check, 2 = failed internal quality check, 3 = reach max allowed iterations, 4 = reached max allowed divergences
retrieved_co2_column	Float32	Retrieved vertical column of CO2
retrieved_dry_air_column_layer_thickness	Float32	Retrieved vertical column of dry air per atmospheric layer
retrieved_h2o_column	Float32	Retrieved vertical column of H2O
retrieved_h2o_column_layer_thickness	Float32	Retrieved vertical column of H2O per atmospheric layer
retrieved_o2_column	Float32	Retrieved vertical column of O2
retrieved_wet_air_column_layer_thickness	Float32	Retrieved vertical column of wet air per atmospheric layer
specific_humidity_profile_ecmwf	Float32	ECMWF specific humidity profile interpolated to observation location, time
surface_pressure_apriori_fph	Float32	Apriori of surface pressure
surface_pressure_fph	Float32	Surface pressure

Element	Type	Comment
surface_pressure_uncert_fph	Float32	Apriori of surface pressure
surface_type	String	"Lambertian" or " Coxmunk,Lambertian" This element can be used to determine whether a sounding is in glint mode (Coxmunk,Lambertian) or nadir (Lambertian).
temperature_offset_apriori_fph	Float32	Apriori of retrieved offset of temperature profile
temperature_offset_fph	Float32	Retrieved offset of temperature profile
temperature_offset_uncert_fph	Float32	Uncertainty of retrieved offset of temperature profile
temperature_profile_met	Float32	Meteorological temperature profile interpolated to observation location, time
tropopause_altitude	Float32	Inferred tropopause altitude based on lapse rate
tropopause_pressure	Float32	Inferred tropopause pressure altitude based on lapse rate";
vector_altitude_levels	Float32	Altitude corresponding to each atmospheric level
vector_altitude_levels_apriori	Float32	A priori altitude corresponding to each atmospheric level"
vector_pressure_levels	Float32	Pressure altitude corresponding to each atmospheric level
vector_pressure_levels_apriori	Float32	A priori pressure altitude corresponding to each atmospheric level";
vector_pressure_levels_met	Float32	Pressure altitude corresponding to each meteorological atmospheric level
wind_speed	Float32	Retrieved Cox-Munk wind speed
wind_speed_apriori	Float32	Apriori of retrieved Cox-Munk wind speed
wind_speed_u_met	Float32	Meteorological eastward wind interpolated to observation location, time
wind_speed_uncert	Float32	Uncertainty of retrieved Cox-Munk wind speed
wind_speed_v_met	Float32	Meteorological northward wind interpolated to observation location, time
xco2	Float32	Column-averaged CO2 dry air mole fraction
xco2_apriori	Float32	Apriori of column-averaged CO2 dry air mole fraction.
xco2_avg_kernel	Float32	Column averaging kernel
xco2_avg_kernel_norm	Float32	Normalized column averaging kernel
xco2_pressure_weighting_function	Float32	Pressure weighting function to form xco2
xco2_uncert	Float32	Error in column averaged target gas dry air mole fraction
xco2_uncert_interf	Float32	Variance of target gas due to interference
xco2_uncert_noise	Float32	Variance of target gas due to noise
xco2_uncert_smooth	Float32	Variance of target gas due to smoothing
zero_level_offset_apriori_o2	Float32	A priori of retrieved zero level offset in O2 band
zero_level_offset_apriori_strong_co2	Float32	A priori of retrieved zero level offset in SCO2 band (not retrieved in the V9 product)
zero_level_offset_apriori_weak_co2	Float32	A priori of retrieved zero level offset in WCO2 band (not retrieved in the V9 product)
zero_level_offset_o2	Float32	Retrieved zero level offset in O2 band
zero_level_offset_strong_co2	Float32	Retrieved zero level offset in SCO2 band (not retrieved in the V9 product)

Element	Type	Comment
zero_level_offset_uncert_o2	Float32	Uncertainty of retrieved zero level offset in O2 band
zero_level_offset_uncert_strong_co2	Float32	Uncertainty of retrieved zero level offset in SCO2 band (not retrieved in the V9 product)
zero_level_offset_uncert_weak_co2	Float32	Uncertainty of retrieved zero level offset in WCO2 band (not retrieved in the V9 product)
zero_level_offset_weak_co2	Float32	Retrieved zero level offset in WCO2 band (not retrieved in the V9 product)

Table 14 describes variables related to the analysis of the three spectral regions. Note that the variables have a Shape including 'Retrieval'. Therefore, soundings are included only when retrievals converged or were converging when the maximum number of iterations was reached.

In the descriptions below, "Reduced chi squared" is defined as:

$$\chi_r^2 = \frac{1}{N_{chan} - 5} \sum_{i=1}^{N_{chan}} \frac{(y_i - f_i(\hat{x})}{\sigma_i^2}$$

where N_{chan} is the number of GOSAT channels in the spectral region, y_i is the radiance value measured by GOSAT in channel i, σ_{i2} is the square of the uncertainty (or noise) in channel i, and $f_i(x)$ is the model of the radiance in channel i.

Table 14: Spectral Parameter Variables

Element	Type	Comment
noise_o2_fph	Float32	
noise_strong_co2_fph	Float32	
noise_weak_co2_fph	Float32	
reduced_chi_squared_o2_fph	Float32	Reduced chi squared of spectral fit for ABO2 spectral region
reduced_chi_squared_strong_co2_fph	Float32	Reduced chi squared of spectral fit for Strong CO2 spectral region
reduced_chi_squared_weak_co2_fph	Float32	Reduced chi squared of spectral fit for Weak CO2 spectral region
relative_residual_mean_square_o2	Float32	Root mean squares of residuals over signal, i.e. sqrt [1/N * Sum[((MeasuredRadiance – ModelRadiance)/signal)^2] where N is the number of spectral elements in the band
relative_residual_mean_square_strong_co2	Float32	Root mean squares of residuals over signal, i.e. sqrt [1/N * Sum[((MeasuredRadiance – ModelRadiance)/signal)^2] where N is the number of spectral elements in the band
relative_residual_mean_square_weak_co2	Float32	Root mean squares of residuals over signal, i.e. sqrt [1/N * Sum[((MeasuredRadiance – ModelRadiance)/signal)^2] where N is the number of spectral elements in the band
residual_mean_square_o2	Float32	Root mean squares of residuals
residual_mean_square_strong_co2	Float32	Root mean squares of residuals

Element	Type	Comment
residual_mean_square_weak_co2	Float32	Root mean squares of residuals
signal_o2_fph	Float32	the signal level representative of the continuum level for this spectrum.
signal_strong_co2_fph	Float32	The signal level representative of the continuum level for this spectrum.
signal_weak_co2_fph	Float32	the signal level representative of the continuum level for this spectrum.
snr_o2_l1b	Float32	Signal-to-noise ratio for ABO2 spectral region . from the L1b processing
snr_strong_co2_l1b	Float32	Signal-to-noise ratio for Strong CO2 spectral region
snr_weak_co2_l1b	Float32	Signal-to-noise ratio for Weak CO2 spectral region

Table 15 describes bit definitions for the three variables that are constructed as bit flags.

Table 15: Bit Flag Definitions

Element	Bit #	Content
l2_packaging_qual_flag	0	Spare
	1	Spare
	2	excluded during sounding selection
	3	skipped due to missing sounding file
	4	skipped due to failed sounding file pre-check
	5	failed due to sounding file read error
	6	Spare
	7	failed due to unexpected packaging error
sounding_qual_flag	0	Radiance calibration 0 = At least one band succeeded at least partially 1 = All three bands failed
	1	Geolocation 0 = Sounding geolocation succeeded 1 = Sounding geolocation failed
	2	Radiance calibration 0 = All three bands succeeded 1 = At least one band failed in at least one color
	3	Sounding geometry 0 = All parameters derived successfully 1 = Derivation failed
	4	Band ABO2 radiance calibration 0 = Successful 1 = At least on one color failed
	5	Band WCO2 radiance calibration 0 = Successful 1 = At least on one color failed
	6	Band SCO2 radiance calibration 0 = Successful 1 = At least on one color failed
	7	Sounding time derivation 0 = Successful 1 = Failed
	8	Derivation of surface parameters using DEM

Element	Bit #	Content
		0 = Successful 1 = Some parameters could not be derived
	9	Spacecraft position and velocity derivation 0 = Successful 1 = Failed
	10-31	Spare

Table 16 describes bit definitions for the three variables that are constructed as bit flags.

Table 16: Fields in the Aerosol Results group of the L2 data products (AerosolResults)

Element	Type	Comment
aerosol_aod	Float32	Retrieved column-integrated aerosol optical depth for column segment: [Total, Low, Med, High]
aerosol_model	FixLenStr	Aerosol model used, if retrieved, one of: [profile_linear, profile_log, linear_aod, gaussian_linear, gaussian_log]
aerosol_param	Float32	Retrieval_AerosolType_AerosolParam_Array
aerosol_param_apriori	Float32	Retrieval_AerosolType_AerosolParam_Array
aerosol_param_uncert	Float32	Retrieval_AerosolType_AerosolParam_Array
aerosol_total_aod	Float32	Retrieved total column-integrated aerosol optical depth for all aerosol types";
aerosol_type_retrieved	Float32	Flag that indicates whether aerosol type was retrieved or not (1 yes, 0 no)

Table 16 describes the fields in the albedo results group of the L2 Standard files.

Table 17: Fields in the Albedo Results group of the L2 data products (AlbedoResults)

Element	Type	Comment
albedo_apriori_o2_fph	Float32	A priori of retrieved Lambertian component of albedo at 0.77 microns
albedo_apriori_strong_co2_fph	Float32	A priori of retrieved Lambertian component of albedo at 2.06 microns
albedo_apriori_weak_co2_fph	Float32	A priori of retrieved Lambertian component of albedo at 1.615 microns
albedo_o2_fph	Float32	Retrieved Lambertian component of albedo at 0.77 microns
albedo_slope_apriori_o2	Float32	A priori of retrieved spectral dependence of Lambertian component of albedo within ABO2 band
albedo_slope_apriori_strong_co2	Float32	A priori of spectral dependence of Lambertian component of albedo within SCO2 band
albedo_slope_apriori_weak_co2	Float32	A priori of retrieved spectral dependence of Lambertian component of albedo within WCO2 band
albedo_slope_o2	Float32	Retrieved spectral dependence of Lambertian component of albedo within ABO2 band
albedo_slope_strong_co2	Float32	Retrieved spectral dependence of Lambertian component of albedo within SCO2 band

Element	Type	Comment
albedo_slope_uncert_o2	Float32	Uncertainty of retrieved spectral dependence of Lambertian component of albedo withint ABO2 band
albedo_slope_uncert_strong_co2	Float32	Uncertainty of spectral dependence of Lambertian component of albedo within SCO2 band
albedo_slope_uncert_weak_co2	Float32	Uncertainty of retrieved spectral dependence of Lambertian component of albedo within WCO2 band
albedo_slope_weak_co2	Float32	Retrieved spectral dependence of Lambertian component of albedo within WCO2 band
albedo_strong_co2_fph	Float32	Retrieved Lambertian component of albedo at 2.06 microns
albedo_uncert_o2_fph	Float32	Uncertainty of retrieved Lambertian component of albedo 0.77 microns
albedo_uncert_strong_co2_fph	Float32	Uncertainty of retrieved Lambertian component of albedo at 2.06 microns
albedo_uncert_weak_co2_fph	Float32	Uncertainty of retrieved Lambertian componet of albedo at 1.615 microns
albedo_weak_co2_fph	Float32	Retrieved Lambertian component of albedo at 1.615 microns

Table 18 describes the fields in the BRDF group.

Table 18: Fields in the BRDF Results group of the L2 data products (BRDFResults)

Element	Type	Comment
brdf_anisotropy_parameter_o2	Float32	RPV kernel anisotropy parameter for ABO2 band (set to 0.75)
brdf_anisotropy_parameter_strong_co2	Float32	RPV kernel anisotropy parameter for SCO2 band (set to 0.75)
brdf_anisotropy_parameter_weak_co2	Float32	RPV kernel anisotropy parameter for WCO2 band (set to 0.75)
brdf_asymmetry_parameter_o2	Float32	RPV kernel asymmetry parameter for ABO2 band (set to -0.1)
brdf_asymmetry_parameter_strong_co2	Float32	RPV kernel asymmetry parameter for SCO2 band (set to -0.1)
brdf_asymmetry_parameter_weak_co2	Float32	RPV kernel asymmetry parameter for WCO2 band (set to -0.1)
brdf_breon_factor_o2	Float32	Amplitude factor applied for Breon part of BRDF for ABO2 band (set to 1e-20)
brdf_breon_factor_strong_co2	Float32	Amplitude factor applied for Breon part of BRDF for SCO2 band (set to 1e-20)
brdf_breon_factor_weak_co2	Float32	Amplitude factor applied for Breon part of BRDF for WCO2 band (set to 1e-20)
brdf_hotspot_parameter_o2	Float32	RPV kernel hotspot parameter for ABO2 band (set to 0.05)
brdf_hotspot_parameter_strong_co2	Float32	RPV kernel hotspot parameter for SCO2 band (set to 0.05)
brdf_hotspot_parameter_weak_co2	Float32	RPV kernel hotspot parameter for WCO2 band (set to 0.05)
brdf_rahman_factor_o2	Float32	Amplitude factor for Rahman (RPV) part of BRDF for ABO2 band (set to 1.0)
brdf_rahman_factor_strong_co2	Float32	Amplitude factor for Rahman (RPV) part of BRDF for SCO2 band (set to 1.0)
brdf_rahman_factor_weak_co2	Float32	Amplitude factor for Rahman (RPV) part of BRDF for WCO2 band (set to 1.0)

Element	Type	Comment
brdf_reflectance_apriori_o2	Float32	A priori of retrieved reflectance, computed from BRDF evaluated at the observation geometry, at 0.77 micron wavelength
brdf_reflectance_apriori_strong_co2	Float32	A priori of retrieved reflectance, computed from BRDF evaluated at the observation geometry, at 2.06 micron wavelength
brdf_reflectance_apriori_weak_co2	Float32	A priori of retrieved reflectance, computed from BRDF evaluated at the observation geometry, at 1.615 micron wavelength
brdf_reflectance_o2	Float32	Retrieved reflectance, computed from BRDF evaluated at the observation geometry, at 0.77 micron wavelength
brdf_reflectance_slope_apriori_o2	Float32	A priori of retrieved spectral dependence of reflectance in ABO2 band
brdf_reflectance_slope_apriori_strong_co2	Float32	A priori of retrieved spectral dependence of reflectance in SCO2 band
brdf_reflectance_slope_apriori_weak_co2	Float32	A priori of retrieved spectral dependence of reflectance in WCO2 band
brdf_reflectance_slope_o2	Float32	Retrieved spectral dependence of reflectance in ABO2 band
brdf_reflectance_slope_strong_co2	Float32	Retrieved spectral dependence of reflectance in SCO2 band
brdf_reflectance_slope_uncert_o2	Float32	Uncertainty of retrieved spectral dependence of reflectance in ABO2 band
brdf_reflectance_slope_uncert_strong_co2	Float32	Uncertainty of retrieved spectral dependence of reflectance in SCO2 band
brdf_reflectance_slope_uncert_weak_co2	Float32	Uncertainty of retrieved spectral dependence of reflectance in WCO2 band
brdf_reflectance_slope_weak_co2	Float32	Retrieved spectral dependence of reflectance in WCO2 band
brdf_reflectance_strong_co2	Float32	Retrieved reflectance, computed from BRDF evaluated at the observation geometry, at 2.06 micron wavelength
brdf_reflectance_uncert_o2	Float32	Uncertainty of retrieved reflectance, computed from BRDF evaluated at the observation geometry, at 0.77 micron wavelength
brdf_reflectance_uncert_strong_co2	Float32	Uncertainty of retrieved reflectance, computed from BRDF evaluated at the observation geometry, at 2.06 micron wavelength
brdf_reflectance_uncert_weak_co2	Float32	Uncertainty of retrieved reflectance, computed from BRDF evaluated at the observation geometry, at 1.615 micron wavelength
brdf_reflectance_weak_co2	Float32	Retrieved reflectance, computed from BRDF evaluated at the observation geometry, at 1.615 micron wavelength
brdf_weight_apriori_o2	Float32	A priori of overall retrieved weight for the composite BRDF, at reference wavelength, for ABO2 band
brdf_weight_apriori_strong_co2	Float32	A priori of overall retrieved weight for the composite BRDF, at reference wavelength, for SCO2 band
brdf_weight_apriori_weak_co2	Float32	A priori of overall retrieved weight for the composite BRDF, at reference wavelength, for WCO2 band
brdf_weight_o2	Float32	Overall retrieved weight for the composite BRDF, at reference wavelength, for ABO2 band
brdf_weight_slope_apriori_o2	Float32	A priori of overall retrieved in-band slope of the weight for the composite BRDF for ABO2 band
brdf_weight_slope_apriori_strong_co2	Float32	A priori of overall retrieved in-band slope of the weight for the composite BRDF for SCO2 band
brdf_weight_slope_apriori_weak_co2	Float32	A priori of overall retrieved in-band slope of the weight for the composite BRDF for WCO2 band

Element	Type	Comment
brdf_weight_slope_o2	Float32	Overall retrieved in-band slope of the weight for the composite BRDF for ABO2 band
brdf_weight_slope_strong_co2	Float32	Overall retrieved in-band slope of the weight for the composite BRDF for SCO2 band
brdf_weight_slope_uncert_o2	Float32	Uncertainty of overall retrieved in-band slope of the weight for the composite BRDF for ABO2 band
brdf_weight_slope_uncert_strong_co2	Float32	Uncertainty of overall retrieved in-band slope of the weight for the composite BRDF for SCO2 band
brdf_weight_slope_uncert_weak_co2	Float32	Uncertainty of overall retrieved in-band slope of the weight for the composite BRDF for SCO2 band
brdf_weight_slope_weak_co2	Float32	Overall retrieved in-band slope of the weight for the composite BRDF for WCO2 band
brdf_weight_strong_co2	Float32	Overall retrieved weight for the composite BRDF, at reference wavelength, for SCO2 band
brdf_weight_uncert_o2	Float32	Uncertainty of overall retrieved weight for the composite BRDF, at reference wavelength, for ABO2 band
brdf_weight_uncert_strong_co2	Float32	Uncertainty of overall retrieved weight for the composite BRDF, at reference wavelength, for SCO2 band
brdf_weight_uncert_weak_co2	Float32	Uncertainty of overall retrieved weight for the composite BRDF, at reference wavelength, for WCO2 band
brdf_weight_weak_co2	Float32	Overall retrieved weight for the composite BRDF, at reference wavelength, for WCO2 band

Table 19 describes the fields in the Dispersion group of the L2 files.

Table 19: Fields in the Dispersion Results group of the L2 data products (DispersionResults)

Element	Type	Comment
dispersion_offset_apriori_o2	Float32	A priori of retrieved dispersion offset term in ABO2 band
dispersion_offset_apriori_strong_co2	Float32	A priori of retrieved dispersion offset term in SCO2 band
dispersion_offset_apriori_weak_co2	Float32	A priori of retrieved dispersion offset term in WCO2 band
dispersion_offset_o2	Float32	Retrieved dispersion offset term in ABO2 band
dispersion_offset_strong_co2	Float32	Retrieved dispersion offset term in SCO2 band
dispersion_offset_uncert_o2	Float32	Uncertainty of retrieved dispersion offset term in ABO2 band
dispersion_offset_uncert_strong_co2	Float32	Uncertainty of retrieved dispersion offset term in SCO2 band
dispersion_offset_uncert_weak_co2	Float32	Uncertainty of retrieved dispersion offset term in WCO2 band
dispersion_offset_weak_co2	Float32	Retrieved dispersion offset term in WCO2 band
dispersion_spacing_apriori_o2	Float32	A priori of retrieved dispersion spacing in ABO2 band
dispersion_spacing_apriori_strong_co2	Float32	A priori of retrieved dispersion spacing in SCO2 band
dispersion_spacing_apriori_weak_co2	Float32	A priori of retrieved dispersion spacing in WCO2 band
dispersion_spacing_o2	Float32	Retrieved dispersion spacing in ABO2 band
dispersion_spacing_strong_co2	Float32	Retrieved dispersion spacing in SCO2 band
dispersion_spacing_uncert_o2	Float32	Uncertainty of retrieved dispersion spacing in ABO2 band
dispersion_spacing_uncert_strong_co2	Float32	Uncertainty of retrieved dispersion spacing in SCO2 band
dispersion_spacing_uncert_weak_co2	Float32	Uncertainty of retrieved dispersion spacing in WCO2 band
dispersion_spacing_weak_co2	Float32	Retrieved dispersion spacing in WCO2 band

Table 20 describes the fields in the IMAP DOAS group of the L2 files.

Table 20: Fields in the IMAP DOAS Preprocessing Results group of the L2 data products (IMAPDOASPreprocessingResults)

Element	Type	Comment
ch4_column_apriori_idp	Float32	A priori Ch4 vertical column density from meteorological forecast
ch4_column_idp	Float32	CH4 vertical column density retrieved from WCO2 band
ch4_column_uncert_idp	Float32	1-sigma error in the CH4 vertical column density from WCO2 band
ch4_weak_band_processing_flag_idp	Signed8	Indicator of whether the CH4 retrieval succeeded: 0 - \'Processing succeeded\', 1 - \'Processing failed\', 2 - \'Processing skipped\', all other values undefined
cloud_flag_idp	Signed8	Cloud flag derived from IMAP-DOAS algorithm: -2 - \'Measurement unusable\', -1 - \'Did not converge\', 0 - \"Definitely cloudy\', 1 - \'Probably cloudy\', 2 - \'Probably clear\', 3 - \'Very clear\', all other values undefined
co2_column_apriori_idp	Float32	A priori CO2 vertical column density from meteorological forecast
co2_column_ch4_window_idp	Float32	CO2 vertical column density retrieved in the CH4 fit window (very weak lines)
co2_column_strong_band_idp	Float32	CO2 vertical column density retrieved from SCO2 band
co2_column_strong_band_uncert_idp	Float32	1-sigma error in the CO2 vertical column density from SCO2 band
co2_column_weak_band_idp	Float32	CO2 vertical column density retrieved from WCO2 band
co2_column_weak_band_uncert_idp	Float32	1-sigma error in the CO2 vertical column density from WCO2 band
co2_ratio_idp	Float32	Ratio of retrieved CO2 column (no scattering code) in WCO2 and SCO2 bands
co2_strong_band_processing_flag_idp	Signed8	Indicator of whether the SCO2 retrieval succeeded: 0 - \'Processing succeeded\', 1 - \'Processing failed\', 2 - \'Processing skipped\', all other values undefined
co2_weak_band_processing_flag_idp	Signed8	ndicator of whether the WCO2 retrieval succeeded: 0 - \'Processing succeeded\', 1 - \'Processing failed\', 2 - \'Processing skipped\', all other values undefined
delta_d_idp	Float32	Deuterium depletion of total column water vapor from retrieved H2O and HDO
delta_d_uncert_idp	Float32	1-sigma uncertainty in deuterium depletion of total column water vapor
dry_air_column_apriori_idp	Float32	Integrated vertical column of dry airmass derived from meteorological forecast
h2o_column_apriori_idp	Float32	A priori H2O vertical column density from meteorological forecast
h2o_column_idp	Float32	Retrieved H2O vertical column density
h2o_column_uncert_idp	Float32	1-sigma error in the H2O vertical column density
h2o_ratio_idp	Float32	Ratio of retrieved H2O column (no scattering code) in WCO2 and SCO2 bands
h2o_ratio_uncert_idp	Float32	1-sigma error in the ratio of retrieved H2O column (no scattering code) in WCO2 and SCO2 bands
hdo_column_apriori_idp	Float32	A priori HDO vertical column density from meteorological forecast
hdo_column_idp	Float32	Retrieved HDO vertical column density
hdo_column_uncert_idp	Float32	1-sigma error in the HDO vertical column density

Element	Type	Comment
hdo_h2o_processing_flag_idp	Signed8	Indicator of whether the HDO-H2O retrieval succeeded: 0 - \'Processing succeeded\', 1 - \'Processing failed\', 2 - \'Processing skipped\', all other values undefined
o2_ratio_p_idp	Float32	Ratio of retrieved and meteorological O2 column, P-polarization
o2_ratio_s_idp	Float32	Ratio of retrieved and meteorological O2 column, S-polarization
out_of_band_transmission_p_idp	Float32	Transmission at the band-pass edge, P-polarization, band 1
out_of_band_transmission_s_idp	Float32	Transmission at the band-pass edge, S-polarization, band 1
total_offset_fit_relative_755nm_p_idp	Float32	Retrieved radiance offset relative to mean radiance in 755nm window, P-polarization
total_offset_fit_relative_755nm_s_idp	Float32	Retrieved radiance offset relative to mean radiance in 755nm window, S-polarization
total_offset_fit_relative_771nm_p_idp	Float32	Retrieved radiance offset relative to mean radiance in 771nm window, P-polarization
total_offset_fit_relative_771nm_s_idp	Float32	Retrieved radiance offset relative to mean radiance in 771nm window, S-polarization

4. ACOS Level 2 Lite Data Products

With this delivery of the ACOS/GOSAT v9 data products, we have released a version of the Lite data files similar to the OCO-2 Lite files. The main differences between the Lite data file are that the files are aggregated on a daily basis, the files contain a streamlined set of output parameters (a subset of the full L2 data products) and they contain warn levels for the retrievals. The warn levels permit users to select the percentage of data to retain, with the "most trusted" soundings offered first. A description of the warn levels is provided in Mandrake et al., 2013. This OCO-2 document provides background information on warn levels and provides details on how warn levels were implemented for OCO-2. They were implemented for the ACOS data in a manner consistent with OCO-2. The primary difference between the OCO-2 implementation and the ACOS implementation of warn levels involves the range of possible values. The ACOS warn levels range from 0 (best quality) to 9 (lowest quality), in OCO-2 v7 data the range runs from 0 to 19. The change to the smaller range will be implemented in the next version of OCO-2 data as well.

Table 21-Table 23 provide a description of the variables available in the Lite data files. They are designed to be somewhat easier to use (smaller files, aggregated daily). The data included in these files are consistent with the Level 2 data products.

Table 21 provides a description of the fields in the ACOS Lite Data Product files.

Element	Type	Comment
co2_profile_apriori	Float32	Prior CO2 Prior assumed by L2 code; Defined on layer boundaries. These are oriented space-to-surface, so the first element defines the TOA, the last element defines the surface.
date	Float32	Observation date and time matching sounding_id.
File_index	Float32	1-Based Index of L2 File for each sounding
latitude	Float32	Center latitude of the measurement
longitude	Float32	Center longitude of the measurement";
levels	Long	Level counter
pressure_levels	Float32	Pressure at each level; Defined on layer boundaries. These are oriented space-to-surface, so the first element defines the TOA, the last element defines the surface
pressure_weight	Float32	Pressure weighting function for each level; Defined on layer boundaries. These are oriented space-to-surface, so the first element defines the TOA, the last element defines the surface
sensor_zenith_angle	Float32	Zenith angle of the satellite at the time of the measurement
solar_zenith_angle	Float32	Solar zenith angle at the time of the measurement
sounding_id	Long	From scan start time in UTC
source_files		Source L2 File Names for these soundings
time	Long	Seconds since 1970-01-01 00:00:00

Element	Type	Comment
xco2	Float32	Column-averaged dry-air mole fraction of CO2 (Bias corrected as described in Section 2.7.3)
xco2_apriori	Float32	A priori Xco2 value
xco2_averaging_kernel	Float32	Xco2 column averaging kernel
xco2_qf_bitflag		ACOS B9 xco2_quality_flag bit flag
xco2_quality_flag	Byte	Xco2 quality flag ("0=Good Retreival, 1=Bad Retrieval)
xco2_uncertainty	Float32	Xco2 posterior error estimate

Table 22 Contains description of the fields in the "Preprocessor" folder of the Lite files.

Element	Type	Comment
co2_ratio	Float32	Band 3 / Band 2 Ratio of retrieved Single-band XCO2 using IMAP-DOAS algorithm
dp_abp	Float32	Retrieved-Prior Pressure from the fast O2A-band only preprocessor retrieval
h2o_ratio	Float32	H2O Ratio
xco2_strong_idp	Float32	XCO2 from Strong CO2 Band only, IMAP-DOAS algorithm
xco2_weak_idp	Float32	XCO2 from Weak CO2 Band only, IMAP-DOAS algorithm

Table 23 Contains description of the fields in the "Retrievals" folder of the Lite files.

Element	Type	Comment
albedo_o2a	float32	Retrieved Band 1 reflectance (land), or lambertian albedo component of BRDF (ocean)
albedo_sco2	float32	Retrieved Band 3 reflectance (land), or lambertian albedo component of BRDF (ocean)
albedo_slope_o2a	float32	Retrieved Band 1 reflectance slope (land), or slope of lambertian albedo component of BRDF (ocean)
albedo_slope_sco2	float32	Retrieved Band 3 reflectance slope (land), or slope of lambertian albedo component of BRDF (ocean)
albedo_slope_wco2	float32	Retrieved Band 2 reflectance slope (land), or slope of lambertian albedo component of BRDF (ocean)
albedo_wco2	float32	Retrieved Band 2 reflectance (land), or lambertian albedo component of BRDF (ocean)
aod_bc	float32	Retrieved Black Carbon Optical Depth at 0.755 microns
aod_dust	float32	Retrieved Dust Aerosol Optical Depth at 0.755 microns
aod_fine	float32	Retrieved Aerosol Fone-Mode Optical Depth at 0.755 microns
aod_ice	float32	Retrieved Ice Cloud Optical Depth at 0.755 microns
aod_oc	float32	Retrieved Organic Carbon Optical Depth at 0.755 microns
aod_seasalt	float32	Retrieved Sea Salt Carbon Optical Depth at 0.755 microns
aod_strataer	float32	Retrieved Upper Trop+Stratospheric Aerosol Optical Depth at 0.755 microns
aod_sulfate	float32	Retrieved Sulfate Aerosol Optical Depth at 0.755 microns

Element	Type	Comment
aod_total	float32	Retrieved Total Cloud+Aerosol Optical Depth at 0.755 microns
aod_water	float32	Retrieved Water Cloud Optical Depth at 0.755 microns
chi2_o2a	float32	Reduced Chi-Squared for Band 1 (O2A band) of L2 spectral fit
chi2_sco2	float32	Reduced Chi-Squared for Band 3 (Strong CO2 band) of L2 spectral fit
chi2_wco2	float32	Reduced Chi-Squared for Band 2 (Weak CO2 band) of L2 spectral fit
co2_grad_del	float32	level 13 is at P/Psurf=0.631579
deltaT	float32	Retrieved Offset to Prior Temperature Profile in Kelvin
diverging_steps	int8	No. of diverging steps taken in retrieval
dp	float32	Retrieved-Prior Pressure from the L2 Full-Physics retrieval
dpfrac	float32	xco2_raw*(1-{Meteorology/psurf_apriori_band3}/{Retrieval/psurf}
dust_height	float32	Retrieved Dust Height
dws	float32	Retrieved AOD_dust+AOD_water+AOD_seasalt at 0.755 microns
eof1_3	float32	Band 1, EOF 3
eof2_3	float32	Band 2, EOF 3
eof3_2	float32	Band 3, EOF 2
eof3_3	float32	Band 3, EOF 3
fs	float32	Simultaneous Fluorescence retrieval (at 757 nm) by L2 code; note this is different than the dedicated retrieval using only solar lines
h2o_scale	float32	Retrieved scale factor to Prior Water Vapor Profile
ice_height	float32	Retrieved Ice Cloud Height
iterations	int8	No. of iterations used in retrieval
lm_param	float32	Value of Levenberg-Marquardt Parameter on final iteration
logDWS	float32	Retrieved max(log(aod_dust+aod_sulfate+aod_ss),-5), at 0.755 microns
psurf	float32	Surface pressure retrieved by the Level-2 retrieval
psurf_apriori	float32	Prior surface pressure used in the retrieval, as determined by ECMWF short-term (0-9 hour) forecast
reduced_chi_squared_per_band	float32	Reduced Chi-Squared for each band (1,2,3) of L2 spectral fit
s31	float32	Ratio of Band 3 to Band 1 signal level
s32	float32	Ratio of Band 3 to Band 2 signal level
SigmaB	float32	Multiply Psurf by these values to get the pressure layer boundaries (= pressure levels)
snr_strong_clip	float32	Band 3 SNR clipped at 600
surface_type	int8	Surface type used in the retrieval: 0=ocean and corresponds to a Coxmunk+Lambertian surface; 1=land and corresponds to a pure Lambertian surface
T700	float32	Temperature at 700 hPa (from ECMWF)
tcwv	float32	Retrieved TCWV obtained by multiplying retrieved h2o_scale factor to prior (ECMWF) TCWV
tcwv_apriori	float32	Prior TCWV (from ECMWF prior profile)
tcwv_uncertainty	float32	Retrieved TCWV Posterior Uncertainty
windspeed	float32	Surface wind speed retrieved by the Level-2 retrieval
windspeed_apriori	float32	Surface wind speed retrieved by the Level-2 retrieval
xco2_raw	float32	Raw value of Retrieved XCO2 (not bias corrected)

Table 24 Contains description of the fields in the "Sounding" folder of the Lite files.

Element	Type	Comment
airmass	float32	Airmass, computed as 1/cos(solar_zenith_angle) + 1/cos(sensor_zenith_angle)
altitude	float32	Surface Altitude in meters above sea level
altitude_stddev	float32	Standard deviation of surface elevation within the FOV
gain	string8	TANSO-FTS gain mode: H is the high-gain mode (used over most of the planet); M is the medium gain mode (used over very bright surfaces)
glint_angle	float32	Angular distance from viewing along the perfect glint direction
l1b_type	int32	
land_fraction	int8	Fraction of the footprint that contains land in percent
path	uint8	GOSAT fixed orbit path number ranging from 1-45
sensor_azimuth_angle	float32	azimuth angle of the satellite at the time of the measurement
snr_o2	float32	O2A-Band Continuum Signal-to-Noise Ratio
snr_strong_co2	float32	Strong CO2-Band Continuum Signal-to-Noise Ratio
snr_weak_co2	float32	Weak CO2-Band Continuum Signal-to-Noise Ratio
solar_azimuth_angle	float32	solar azimuth angle at the time of the measurement

Table 25: Fields in the "Meteorology" folder of the ACOS/GOSAT Lite files.

Element	Type	Comment
windspeed_u_met	float32	Apriori Surface Wind Speed, U Componentfrom GEOS-5 FPIT in the N-S direction, m/s
windspeed_v_met	float32	Apriori Surface Wind Speed, V Component from GEOS-5 FPIT in the E-W direction, m/s

5. Tools and Data Services

5.1. HDFView

HDFView is a Java based graphical user interface created by the HDF Group that can be used to browse all ACOS HDF products. The utility allows users to view all objects in an HDF file hierarchy, which is represented as a tree structure. HDFView can be downloaded or support found at: https://portal.hdfgroup.org/display/support/Download+HDFView

5.2. Panoply.

Panoply is a tool from the Goddard Institute for Space Studies (GISS). It plots geo-referenced and other arrays from netCDF, HDF, GRIB, and other datasets. Panoply is a cross-platform application that runs on Macintosh, Windows, Linux and other desktop computers. A particularly convenient feature of Panoply is its ability to communicate with remote Hyrax (xml) catalogues and thus plotting datasets without the need to download the data files. Apart from the on-line archive, Goddard DAAC serves ACOS and OCO data through Hyrax (OPeNDAP) as well, and this path to data can be discovered in the ACOS and OCO dataset landing pages (see below). Panoply is available for free download from the GISS website.

5.3. Goddard DAAC user interface.

The NASA Goddard DAAC provides temporal and spatial searches, as well as variable and spatial subsets, through its user interface. Dataset landing pages provide basic summary and data access points for all datasets curated by the DAAC. A simple keyword search would suffice to discover all ACOS datasets:

https://disc.gsfc.nasa.gov/datasets?keywords=ACOS

Apart from the direct access to the online archive and Hyrax (OPeNDAP) directories, the interface ultimately provides the search results as lists of data links. Goddard DAAC requires **user registration** before any data can be downloaded. Detailed instructions on how to register and how to use wget and curl with the data download links, as well as other advanced methods, are provided on the interface:

https://disc.gsfc.nasa.gov/data-access#

5.4. NASA Earth Data Search Client

In a similar manner, information and data access can be found from the NASA Earth Data Search Client:

https://search.earthdata.nasa.gov/search?q=acos

All NASA data centers from the Earth Science Data Information System (ESDIS) report their data collections to this system. It is a convenient one-stop shop for discovery of all NASA Earth Science Missions data.

6. Contact Information

Contact information of the producer of the data products:

ACOS operations team: sdosops@nephthys.jpl.nasa.gov

Contact information for interpretation and usage of the data products:

ACOS data team: acos@jpl.nasa.gov

The following list is of related organizations, web sites or publications that may be beneficial to the user.

- Japanese Aerospace Exploration Agency:
  - http://www.jaxa.jp/projects/sat/gosat/index_e.html
- Japanese National Institute for Environmental Studies:
  - http://www.gosat.nies.go.jp/index_e.html

7. Acknowledgements, References and Documentation

7.1. Acknowledgements

This research was carried out at the Jet Propulsion Laboratory, California Institute of Technology, under a contract with the National Aeronautics and Space Administration.

Figures 5 and 6 are taken from the JAXA press release "Greenhouse Gases Observing Satellite "IBUKI" (GOSAT) "First Light" Acquired by Onboard Sensors", February 9, 2009 (JST).

7.2. Links

The following list provides references to relevant documentation that users may find helpful.

- General GOSAT information:
  - http://www.jaxa.jp/projects/sat/gosat/index_e.html
  - http://www.gosat.nies.go.jp/index_e.html
  - http://www.gosat.nies.go.jp/eng/GOSAT_pamphlet_en.pdf
- Level 2 algorithm information:
  - ACOS Level 2 Algorithm Theoretical Basis Document, JPL D-65488
- Releases and publications:
  - http://www.jaxa.jp/press/2009/02/20090209_ibuki_e.html

7.3. References

7.3.1. GOSAT

Japan Aerospace Exploration Agency (2018), Release Notes for GOSAT FTS Level 1 Products (Ver.210.210), SAM-170119.

Kataoka, F. et al. (2017), The Cross-Calibration of Spectral Radiances and Cross-Validation of CO2 Estimates from GOSAT and OCO-2, Remote Sensing, DOI: 10.3390/rs9111158.

Kataoka, F. et al. (2019), Calibration, Level 1 Processing, and Radiometric Validation for TANSO-FTS TIR on GOSAT, IEEE Trans. Geos. Rem. Sens., DOI: 10.1109/TGRS.2018.2885162.

Kuze, A., et al.(2016), Update on GOSAT TANSO-FTS performance, operations, and data products after more than six years in space, Atmos. Meas. Tech., doi:10.5194/amt-2015-333, Volume: 9, 6, 2445-2461, 2016.

Saitoh, N. et al.(2017), Bias assessment of lower and middle tropospheric CO2 concentrations of GOSAT/TANSO-FTS TIR version 1 product, Atmos. Meas. Tech., DOI: 10.5194/amt-10-3877-2017.

Tanaka, T. et al.(2016), Two-Year Comparison of Airborne Measurements of CO2 and CH4 With GOSAT at Railroad Valley, Nevada, DOI: 10.1109/TGRS.2016.2539973.

7.3.2. OCO-2 Mission

Canadell, J.G., C. Le Quere, M.R. Raupach, C.B. Field, E.T. Buitenhuis, P. Ciais, T.J. Conway, N.P. Gillett, R.A. Houghton, and G. Marlan (2007), Contributions to accelerating

atmospheric CO2 growth from economic activity, carbon intensity, and efficiency of natural sinks, *Proceedings of the National Academy of Sciences*, 47, 18866-18870.

Conway, T.J., P.M. Lang, and K.A. Masarie (2011), Atmospheric carbon dioxide dry air mole fractions from the NOAA ESRL carbon cycle cooperative global air sampling network, 1968-2010, Version: 2011-10-14, http://www.esrl.noaa.gov/gmd/ccgg/trends/global.html

Buchwitz, M., Schneising, O., Burrows, J. P., Bovensmann, H., Reuter, M., and Notholt, J. (2007), First direct observation of the atmospheric CO2 year-to-year increase from space, *Atmos. Chem. Phys.*, 7, 4249–4256, doi:10.5194/acp-7-4249-2007,

Crisp, D., R.M. Atlas, F.-M. Breon, L.R. Brown, J.P. Burrows, P. Ciais, B.J. Connor, S.C. Doney, I.Y. Fung, D.J. Jacob, C.E. Miller, D. O'Brien, S. Pawson, J.T. Randerson, P. Rayner, R.J. Salawitch, S.P. Sander, B. Sen, G.L. Stephens, P.P. Tans, G.C. Toon, P.O. Wennberg, S.C. Wofsy, Y.L. Yung, Z. Kuang, B. Chudasama, G. Sprague, B. Weiss, R. Pollock, D. Kenyon, S. Schroll (2004), The Orbiting Carbon Observatory (OCO) mission, *Advances in Space Research* 34 700–709.

Crisp, D., C. E. Miller, and P. L. DeCola (2008), NASA Orbiting Carbon Observatory: Measuring the column averaged carbon dioxide mole fraction from space, *JARS*.

Frankenberg, C., Chris O'Dell, Joseph Berry, Luis Guanter, Joanna Joiner, Philipp Köhler, Randy Pollock, Thomas E. Taylor (2014a), Prospects for chlorophyll fluorescence remote sensing from the Orbiting Carbon Observatory-2, *Remote Sensing of Environment*, 147, 1-12.

Frankenberg, C., R. Pollock, R. A. M. Lee, R. Rosenberg, J.-F. Blavier, D. Crisp, C.W. O'Dell, G. B. Osterman, C. Roehl, P. O. Wennberg, and D. Wunch (2014b), The Orbiting Carbon Observatory (OCO-2): spectrometer performance evaluation using prelaunch direct Sun measurements, *Atmos. Meas. Tech.*, 7, 1–10. www.atmos-meas-tech.net/7/1/2014/doi:10.5194/amt-7-1-2014.

Hamazaki, T., Kaneko, Y., Kuze, A., and Kondo, K. (2005), Fourier transform spectrometer for greenhouse gases observing satellite (GOSAT), in: *Proceedings of SPIE*, vol. 5659, p. 73-80, doi: 10.1117/12.581198.

Kuze. A., Suto. H., Nakajima, M., and Hamazaki, T. (2009), Thermal and near infrared sensor for carbon observation Fourier-transform spectrometer on the Greenhouse Gases Observing Satellite for greenhouse gases monitoring, *Appl. Opt.*, 48, 6716–6733, 15 doi:10.1364/AO.48.006716

Kuze, A, T. E. Taylor, F. Kataoka, C. J. Bruegge, D. Crisp, M. Harada, M. Helmlinger, M. Inoue, S. Kawakami, N. Kikuchi, Y. Mitomi, J. Murooka, M. Naitoh, D. M. O'Brien, C. W. O'Dell, H. Ohyama, H. Pollock, F. M. Schwandner, K. Shiomi, H. Suto, T. Takeda, T. Tanaka, T. Urabe, T. Yokota, and Y. Yoshida, (2014), Long-Term Vicarious Calibration of GOSAT Short-Wave Sensors: Techniques for Error Reduction and New Estimates of Radiometric Degradation Factors, *IEEE Transactions On Geoscience and Remote Sensing*, 52, 3991-4004, doi:10.1109/TGRS.2013.2278696.

Le Quéré, C., G. P. Peters, R. J. Andres, R. M. Andrew, T. A. Boden, P. Ciais, P. Friedlingstein, R. A. Houghton, G. Marland, R. Moriarty, S. Sitch, P. Tans, A. Arneth, A. Arvanitis, D. C. E. Bakker, L. Bopp, J. G. Canadell, L. P. Chini, S. C. Doney, A. Harper, I. Harris, J. I. House, A. K. Jain, S. D. Jones, E. Kato, R. F. Keeling, K. Klein Goldewijk, A. Körtzinger, C. Koven, N. Lefèvre, F. Maignan, A. Omar, T. Ono, G.-H. Park, B. Pfeil, B. Poulter, M. R. Raupach,*, P. Regnier, C. Rödenbeck, S. Saito, J. Schwinger, J. Segschneider, B. D. Stocker, T. Takahashi, B. Tilbrook, S. van Heuven, N. Viovy, R. Wanninkhof, A.

Wiltshire, and S. Zaehle, (2014), Global carbon budget 2013, *Earth Syst. Sci. Data*, 6, 235–263, www.earth-syst-sci-data.net/6/235/2014/ doi:10.5194/essd-6-235-2014.

P.J. Rayner and D.M. O'Brien (2001), The utility of remotely sensed CO2 concentration data in surface source inversions, *Geophys. Res. Lett*. 28, 175-178.

Yoshida, Y., Ota, Y., Eguchi, N., Kikuchi, N., Nobuta, K., Tran, H., Morino, I., and Yokota, T.: (2011), Retrieval algorithm for CO_2 and CH_4 column abundances from short-wavelength infrared spectral observations by the Greenhouse Gases Observing Satellite, *Atmos. Meas. Tech.*, 4, 717–734, doi:10.5194/amt-4-717-2011.

7.3.3. Algorithms and Retrievals

Crisp, D., B. M. Fisher, C.W. O'Dell, C. Frankenberg, R. Basilio, H. Bösch, L. R. Brown, R. Castano, B. Connor, N. M. Deutscher, A. Eldering, D. Griffith, M. Gunson, A. Kuze, L. Mandrake, J. McDuffie, J. Messerschmidt, C. E. Miller, I. Morino, V. Natraj, J. Notholt, D. O'Brien, F. Oyafuso, I. Polonsky, J. Robinson, R. Salawitch, V. Sherlock, M. Smyth, H. Suto, T. Taylor, P. O. Wennberg, D. Wunch, and Y. L. Yung (2012), The ACOS X_{CO2} retrieval algorithm, Part 2: Global X_{CO2} data characterization. *Atmos Meas. Tech.*, 5, 687-707.

Frankenberg, C., Platt, U., and Wagner, T. (2005), Iterative maximum *a posteriori* (IMAP-) DOAS for retrieval of strongly absorbing trace gases: Model studies for CH4 and CO2 retrieval from near- infrared spectra of SCIAMACHY onboard ENVISAT, *Atmos. Chem. Phys.*, 5, 9–22.

Lee et al. (2015), Preflight Spectral Calibration of the Orbiting Carbon Observatory-2, in preparation.

Mandrake, L., C. Frankenberg, C. W. O'Dell, G. Osterman, P. Wennberg and D. Wunch (2013), Semi-autonomous sounding selection for OCO-2, *Atmos. Meas. Tech., 6*, 2851-2864.

O'Dell, C.W., B. Connor, H. Bösch, D. O'Brien, C. Frankenberg, R. Castano, M. Christi, D. Crisp, A. Eldering, B. Fisher, M. Gunson, J. McDuffie, C. E. Miller, V. Natraj, F. Oyafuso, I. Polonsky, M. Smyth, T. Taylor, G. C. Toon, P. O. Wennberg, and D. Wunch, (2012), The ACOS CO2 retrieval algorithm, Part 1: Description and validation against synthetic observations. *Atmos. Meas. Tech.*, 5, 99-121.

O'Dell, C.W., et al (2018): Improved Retrievals of Carbon Dioxide from the Orbiting Carbon Observatory-2 with the version 8 ACOS algorithm, *Atmos. Meas. Tech. Discuss.*, https://doi.org/10.5194/amt-2018-257,.

Rodgers, C. (2000) Inverse Methods for Atmospheric Sounding: Theory and Practice. World Scientific Publishing Co Pte Ltd.

Taylor, T.E., C. O'Dell, D.M. O'Brien, N. Kikuchi, T. Yokota, T. Nakajima, H. Ishida, D. Crisp, and T. Nakajima (2011), Comparison of cloud screening methods applied to GOSAT near-infrared spectra, IEEE *Trans. Geosci. Rem. Sens*., doi: 10.1109/TGRS.2011.2160270.

Taylor, T.E., C. O'Dell, D.M. O'Brien, N. Kikuchi, T. Yokota, T. Nakajima, H. Ishida, D. Crisp, and T. Nakajima (2011), Comparison of cloud screening methods applied to GOSAT near-infrared spectra, IEEE *Trans. Geosci. Rem. Sens*., doi: 10.1109/TGRS.2011.2160270.

Taylor, T.E., C.W. O'Dell, C. Frankenberg, P. Partian, H. W. Cronk, A. Savtchenko, H. R. Pollock, D. Crisp, A. Eldering, and M. Gunson, (2015), Orbiting Carbon Observatory-2 (OCO-2) aerosol and cloud screening; validation against collocated MODIS data, manuscript in preparation.

7.3.4. Chlorophyll Fluorescence

Frankenberg, C., Fisher, J., Worden, J., Badgley, G., Saatchi, S., Lee, J.-E., et al. (2011), New global observations of the terrestrial carbon cycle from GOSAT: Patterns of plant fluorescence with gross primary productivity. *Geophysical Research Letters*, 38(17), L17706.

Frankenberg, C., O'Dell, C., Guanter, L., & McDuffie, J. (2012), Remote sensing of near-infrared chlorophyll fluorescence from space in scattering atmospheres: implications for its retrieval and interferences with atmospheric CO2 retrievals. *Atmospheric Measurement Techniques*, 5(8), 2081–2094, doi: 10.5194/amt-5-2081-2012.

Joiner, J., Y. Yoshida, A. P. Vasilkov, Y. Yoshida , L. A. Corp , and E. M. Middleton (2011), First observations of global and seasonal terrestrial chlorophyll fluorescence from space, *Biogeosciences*, 8, 637–651.

7.3.5. Validation and TCCON

Deutscher N. et al. (2010), Total column CO2 measurements at Darwin, Australia - site description and calibration against in situ aircraft profiles, Atmos. Meas. Tech., 3, 947–958, doi:10.5194/amt-3-947-2010.

Frankenberg C. et al. (2016), Using airborne HIAPER Pole-to-Pole Observations (HIPPO) to evaluate model and remote sensing estimates of atmospheric carbon dioxide, *Atmos. Chem. Phys.*, 16, 7867-7878, DOI: 10.5194/acp-16-7867-2016.

Keppel-Aleks G. et al. (2011), Sources of variations in total column carbon dioxide, Atmospheric Chemistry and Physics, 11, 3581–3593, doi:10.5194/acp-11-3581-2011, http://www.atmos-chem-phys.net/11/3581/2011/, 2011.

Kiel M. et al. (2019), How bias correction goes wrong: measurement of X-CO2 affected by erroneous surface pressure estimates, 12, https://doi.org/10.5194/amt-12-2241-2019.

Kulawik S. et al. (2015), Consistent evaluation of GOSAT, SCIAMACHY, CarbonTracker, and MACC through comparisons to TCCON, Atmos. Meas. Tech. Discuss., 8, 6217-6277, doi:10.5194/amtd-8-6217-2015.

Lindqvist H. et al. (2015), Does GOSAT capture the true seasonal cycle of carbon dioxide?, Atmos. Chem. Phys., 15, 13023-13040, doi:10.5194/acp-15-13023-2015.

Messerschmidt et al. (2011), Calibration of TCCON column-averaged CO2: the first aircraft campaign over European TCCON sites, Atmos. Chem. Phys. Discuss., 11, 14 541–14 582, doi:10.5194/acpd-11-14541-2011.

Washenfelder R. et al. (2006), Carbon dioxide column abundances at the Wisconsin Tall Tower site, *J. Geophys. Res*, 111, D22305, doi: 10.1029/2006JD007154.

Wunch D. et al. (2010), Calibration of the Total Carbon Column Observing Network using aircraft profile data, *Atmospheric Measurement Techniques*, 3, 1351–1362, doi: 10.5194/amt-3-1351-2010, http://www.atmos-meas-tech.net/3/1351/2010.

Wunch D. et al. (2011a), The Total Carbon Column Observing Network, *Phil. Trans. R. Soc. A*, 369, 2087–2112, doi: 10.1098/rsta.2010.0240.

Wunch D. et al. (2011b), A method for evaluating bias in global measurements of CO_2 total columns from Space, *Atmos. Chem. Phys. Discuss.*, *11*, 20899-20946.

Wunch D. et al. (2017), Comparisons of the Orbiting Carbon Observatory-2 (OCO-2) X_{CO2} Measurements with TCCON, *Atmos. Meas. Tech. Discuss.*, *10*, 2209-2238.